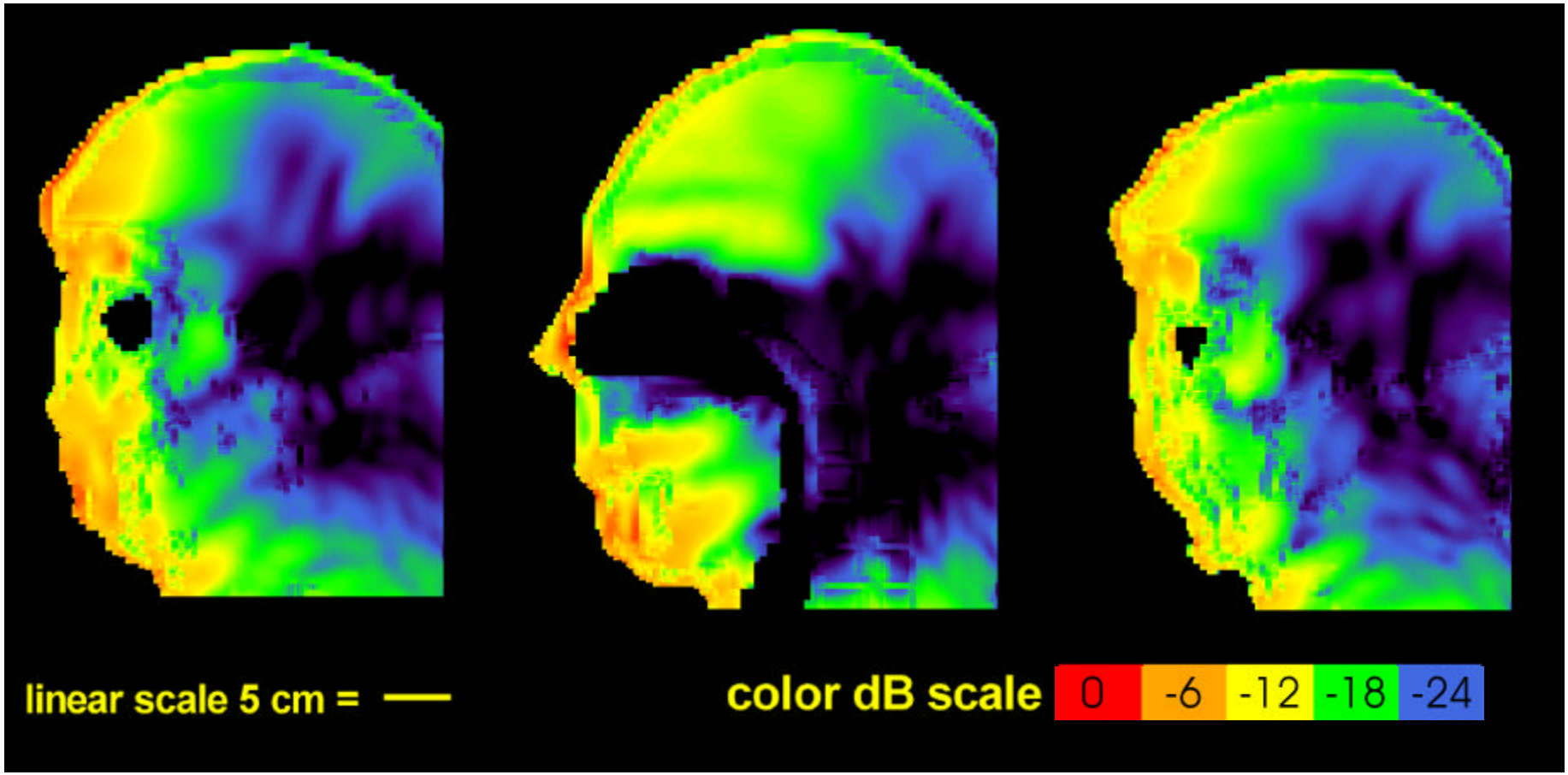

scan L, slice 120
0 dB = 0.177 W/kg

scan M, slice 154
0 dB = 0.180 W/kg

scan N, slice 190
0 dB = 0.190 W/kg

Figure 7.1. FDTD derived x-z plane SAR distributions (L-N) in REMCOM model head exposed to AT&T RU Antenna with tip of nose in contact with radome and centered over middle of patch array.

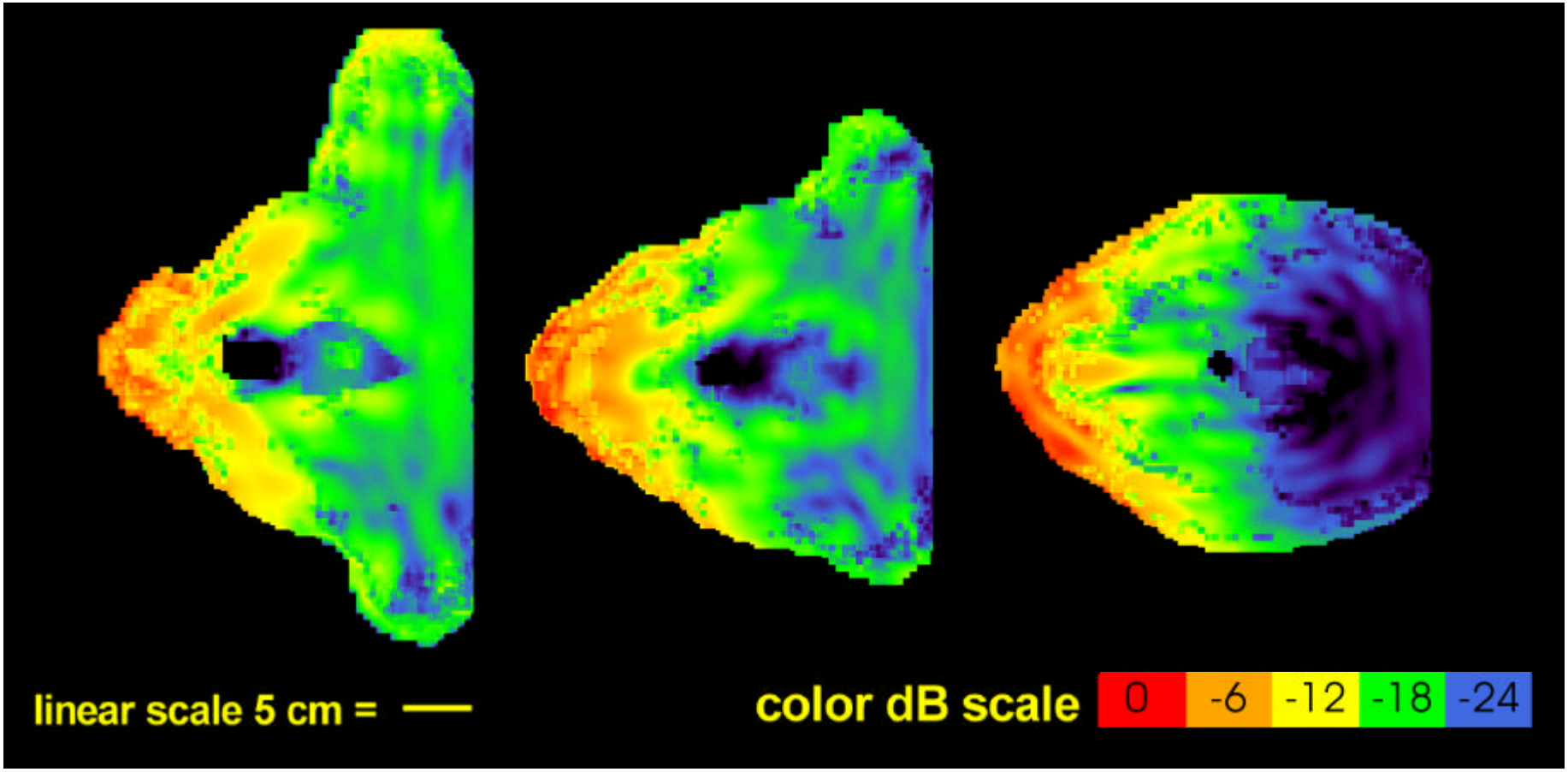

scan A, slice 95
0 dB = 0.1023 W/kg

scan B, slice 105
0 dB = 0.1050 W/kg

scan D, slice 140
0 dB = 0.09087 W/kg

Figure 7.2. FDTD derived x-y plane SAR distributions (A-D) in REMCOM model head exposed to AT&T RU antenna with tip of nose in contact with radome and centered over middle of patch array.

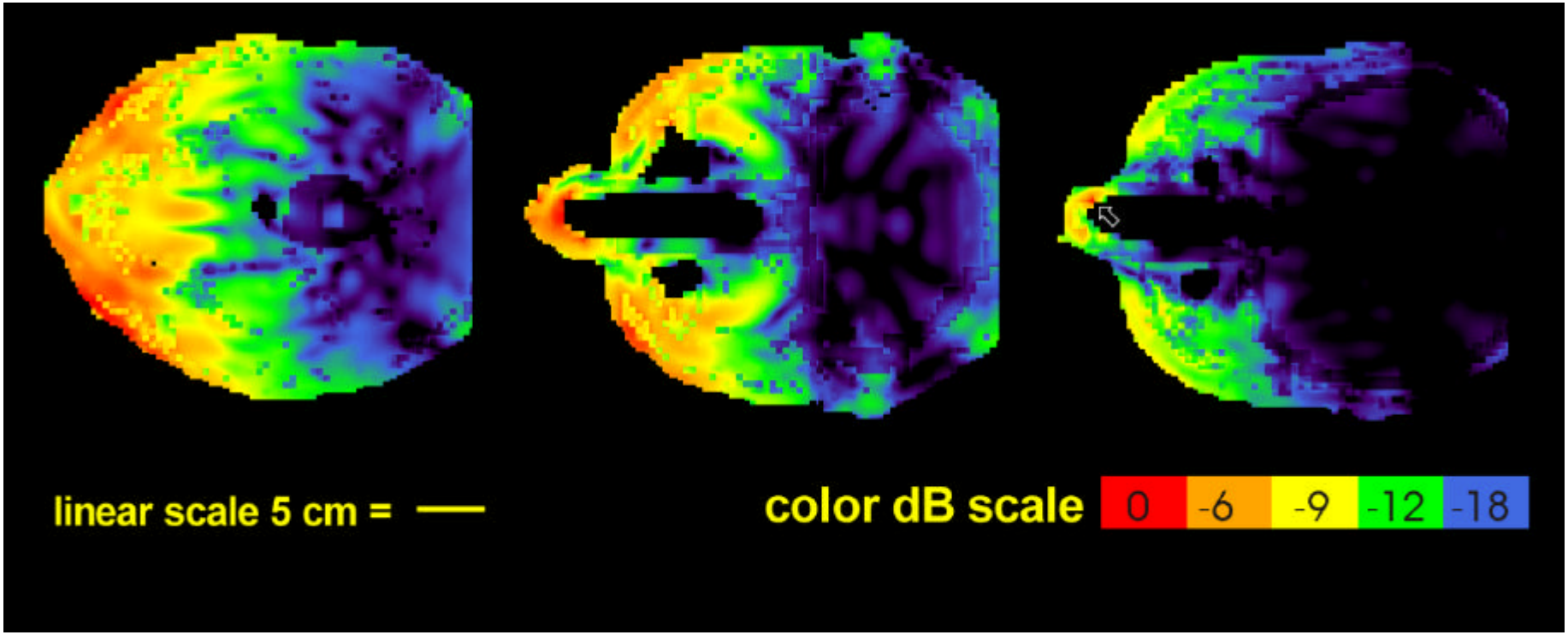

scan E, slice 160
0 dB = 0.06055 W/kg

scan F, slice 193
0 dB = 0.08553 W/kg

scan G, slice 213
0 dB = 0.4388 W/kg

Figure 7.3. FDTD derived x-y plane SAR distributions (E-G) in REMCOM model head exposed to AT&T RU antenna with tip of nose in contact with radome and centered over middle of patch array, (white arrow points to position of maximum SAR for entire head).

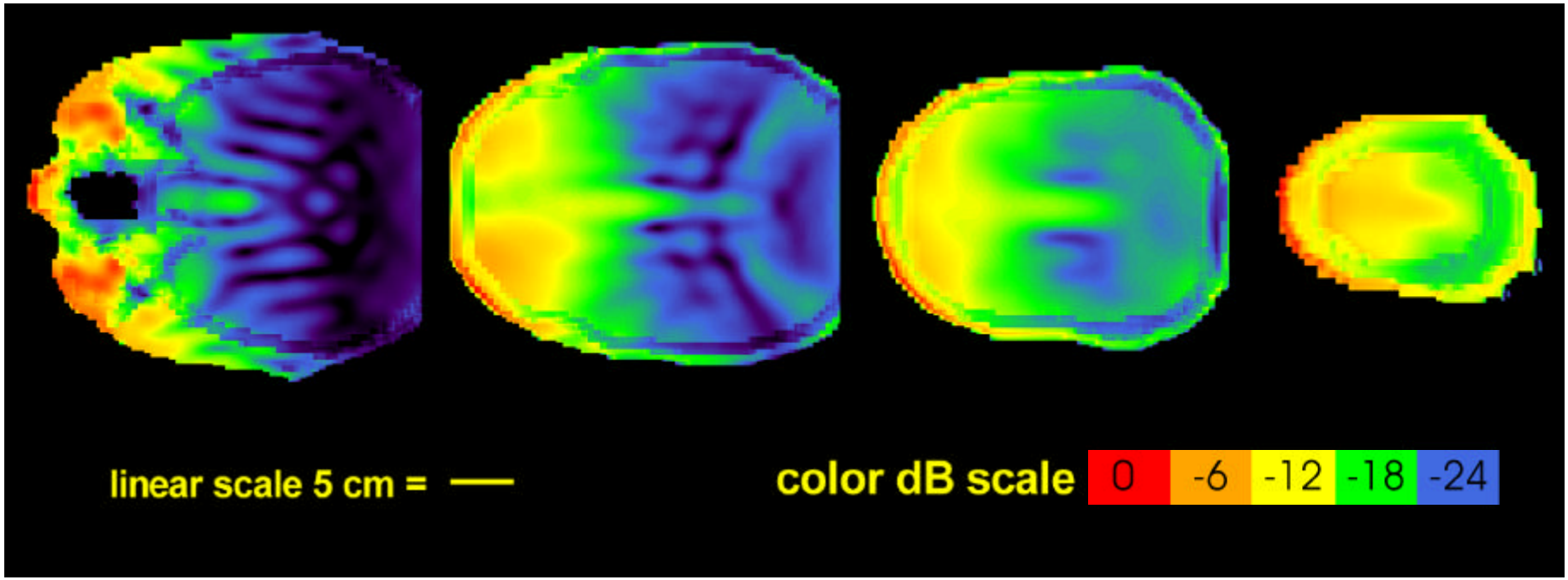

scan H, slice 231
0 dB = 0.1045 W/kg

scan I, slice 260
0 dB = 0.171 W/kg

scan J, slice 290
0 dB = 0.1693 W/kg

scan K, slice 315
0 dB = 0.05614 W/kg

Figure 7.4. FDTD derived x-y plane SAR distributions (H-K) in REMCOM model head exposed to AT&T RU antenna with tip of nose in contact with radome and centered over middle of patch array.

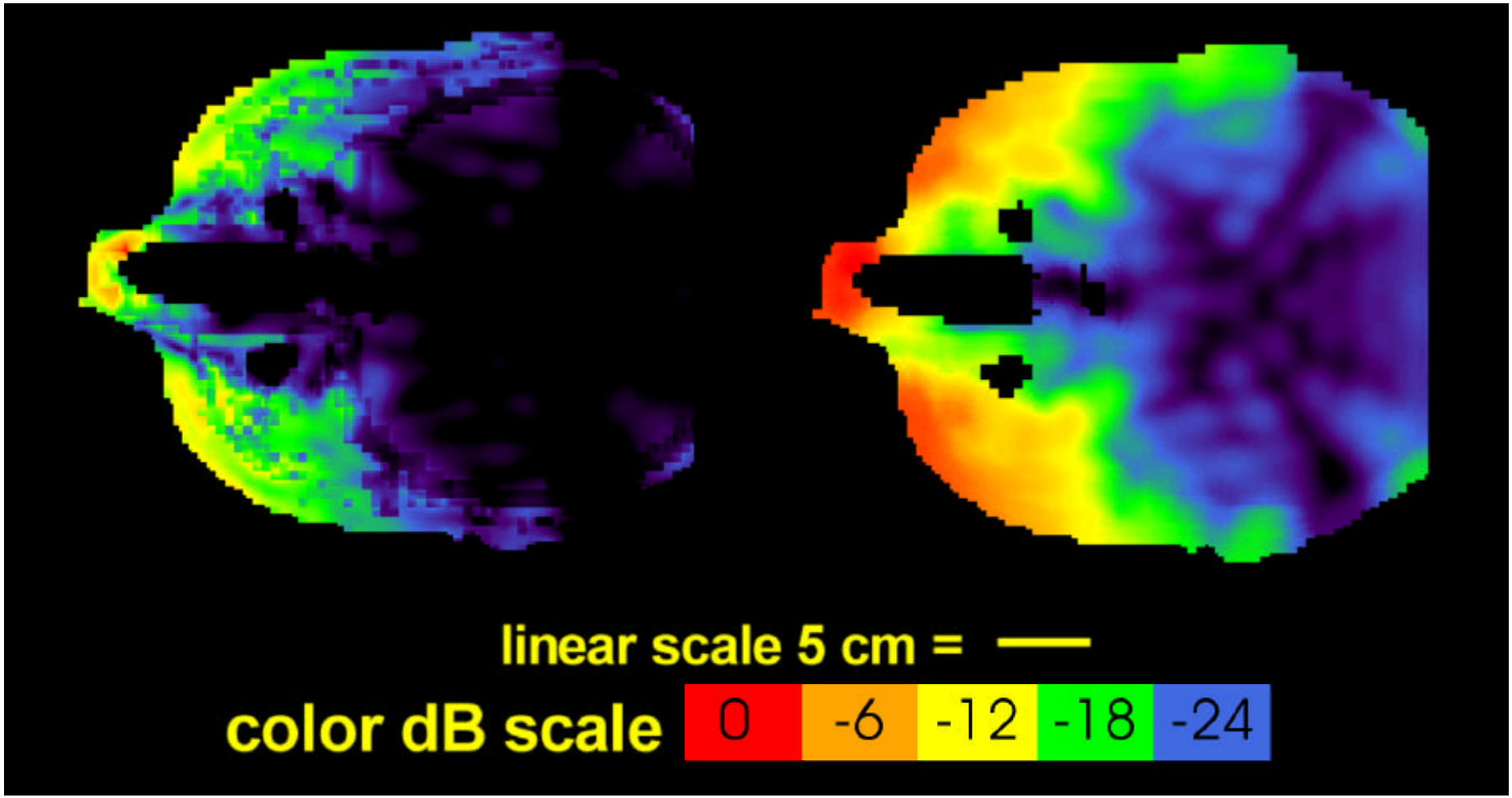

peak SAR = 0.4388 W/kg Maximum 1 gram average SAR = 0.05347 W/kg

Figure 7.5. Slice 213 in x-y plane containing highest FDTD derived peak SAR in REMCOM model head exposed to AT&T RU antenna with tip of nose in contact with radome and centered over middle of patch array (peak due to artifact from sharp corner produced by cubical voxels at air interface within nose shown in left distribution which is discounted with 1 gram averaging shown in right distribution).

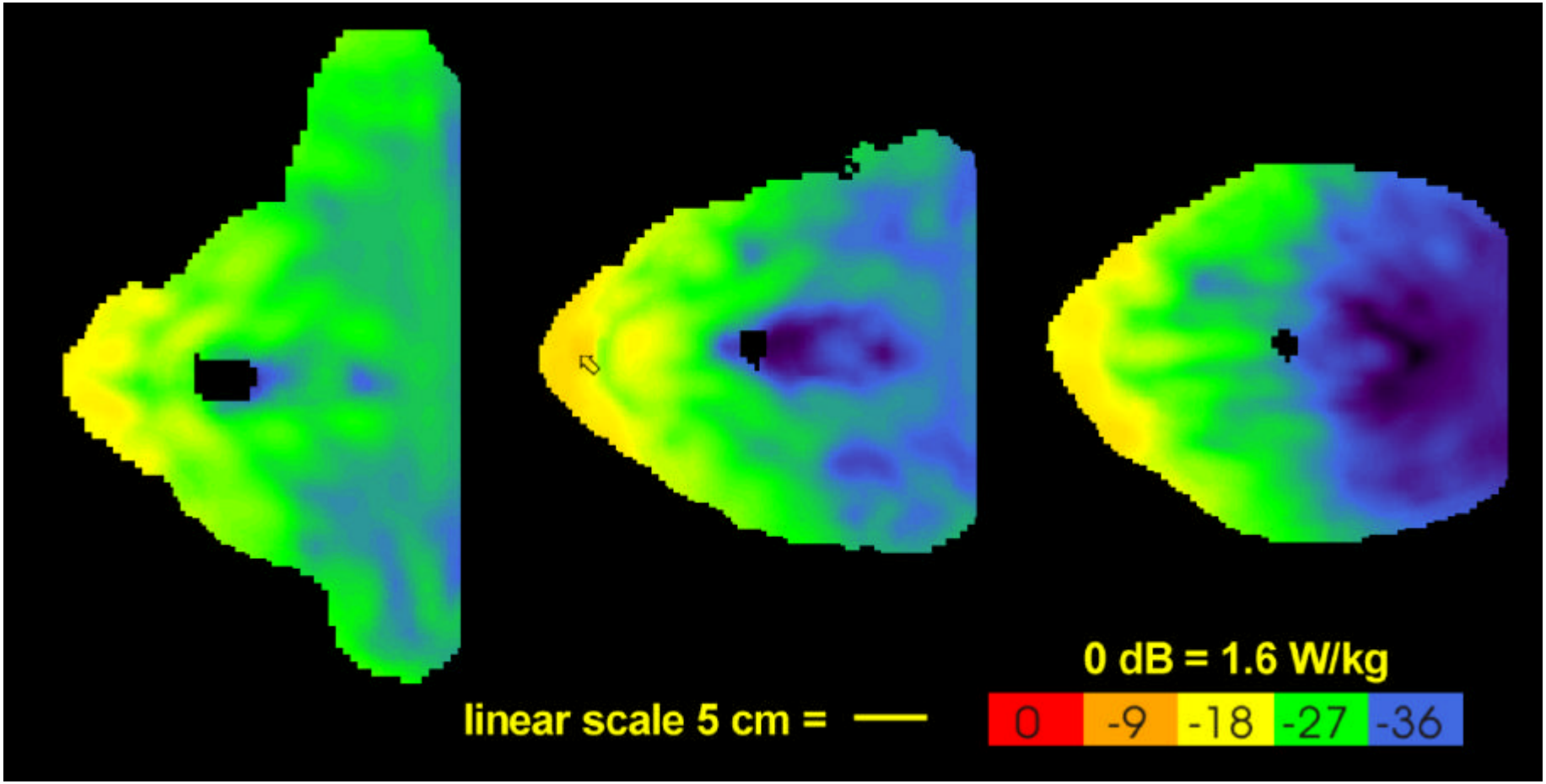

scan A, slice 95
Max. = 0.03513

scan B, slice 113
Max. = 0.06860

scan D, slice 140
Max. = 0.04946

Figure 7.6. FDTD derived x-y plane 1 gram average SAR (W/kg) distributions (A-D) in REMCOM model head exposed to AT&T RU antenna with tip of nose in contact with radome and centered over middle of patch array compared to maximum allowed by FCC MPL (black arrow indicates position of maximum 1 g average SAR for entire head).

8 FDTD Calculation of SAR in Inhomogeneous Rectangular Slab Torso Model

FDTD calculations were made of the peak and 1-gram average of the SARs in the inhomogeneous slab model of the human torso (described in section 3.4) exposed to the AT&T RU antenna. The model was exposed with the skin surface toward the antenna and in direct contact with the radome centered in front of the antenna. Graphical SAR data files and plots calculated throughout the entire slab model was scaled to correspond to an input power of 79.62 mW. At a time when majority of the calculations based on power fed to both coaxial input connectors were completed for this report, it was decided by the ATTWS engineers that the AT&T RU antenna would be fed with the full power applied to the bottom feed connector only, reserving the top feed connector for receiving. There was a question of whether the antenna near field patterns would change, resulting in different SAR patterns and levels in exposed subjects. Clearly if the power is doubled in the bottom conductor, the fields associated with the striplines connected to those feeds would increase by a factor of the square root of 2 resulting in a higher SAR in the tissues exposed to those fields. On-the-other-hand if the feed radiation is low and the power is distributed evenly to the four radiating patch elements, the radiation and the SAR resulting from exposure to those elements should be the same. If it can be demonstrated that the SAR magnitude and distribution at and near the surface of the slab model exposed to the RU antenna is essentially the same for both the single feed and the double feed configured antenna, we need not repeat the calculations for the other models. Thus SAR calculations were made for the inhomogeneous slab model exposed to both the single and the double feed antennas.

8.1 Exposure to Double Feed Antenna

Table 8.1 summarizes the calculated results of both the peak and average SARs calculated for each 1-mm thick slice in the xz plane as well as for the entire exposed slab model. The format of the table is the same as that for Tables 6.1, 6.3 and 6.5 as explained in the previous sections of this report. It may be noted from the table that the maximum SAR of 0.8051 W/kg for the entire slab model is in the 231st slice (file slab.xz231.sar) at x=49 mm and z=139 mm at the surface of the skin layer and the average SAR for the 55998 cells for that slice is 0.008213 W/kg. It can also be seen at the bottom of the table that the SAR as averaged over the 15567443 cells of the entire slab model is 0.004233 W/kg.

Table 8.2 illustrates the results of the 1-gram averaging of the FDTD output

data, which can be related to the FCC MPL. It may be noted from the table that the highest 1-gram average SAR of 0. 3464 W/kg occurs in the slice at z=232 mm, x=48 mm and z=140 mm. This is 6.6 dB below FCC MPL of 1.6 W/kg. Using the same procedure as outlined in the previous section for the homogeneous head, the total absorbed power is calculated to be 65.590 mW, which is 82.9% of the antenna, input power. Thus the whole-body averaged SAR for an adult man with a torso similar to that of the slab model would be somewhere between 0.001377 and 0.004233 W/kg or from 19 to 58 times less than that allowed by the FCC MPL of 0.08 W/kg.

Table 8.1. Slice and Whole Slab Model Peak and average SAR (averaged over slice) for Inhomogeneous Slab Model Exposed to AT&T RU Antenna with Surface of Skin in Contact with Radome and centered with Middle of Patch Array (xz-plane slice file number is distance in mm from FDTD space rectangular coordinates origin in y direction).

Name of Slice Data File	Peak SAR x and z coordinates		Peak SAR (W/kg)	Avg. SAR (W/kg)	Voxels in tissue
slabs.xz15.sar	48	98	0.5375E-01	0.7919E-03	55998
slabs.xz16.sar	48	98	0.6003E-01	0.9261E-03	55998
slabs.xz17.sar	48	98	0.6451E-01	0.1063E-02	55998
slabs.xz18.sar	48	97	0.6750E-01	0.1200E-02	55998
slabs.xz19.sar	48	237	0.7015E-01	0.1333E-02	55998
slabs.xz20.sar	48	237	0.7648E-01	0.1461E-02	55998
slabs.xz21.sar	48	159	0.8308E-01	0.1580E-02	55998
slabs.xz22.sar	48	158	0.8996E-01	0.1690E-02	55998
slabs.xz23.sar	48	157	0.9684E-01	0.1789E-02	55998
slabs.xz24.sar	48	157	0.1039E+00	0.1878E-02	55998
slabs.xz25.sar	48	156	0.1111E+00	0.1957E-02	55998
slabs.xz26.sar	48	155	0.1186E+00	0.2027E-02	55998
slabs.xz27.sar	48	155	0.1265E+00	0.2090E-02	55998
slabs.xz28.sar	48	154	0.1348E+00	0.2146E-02	55998
slabs.xz29.sar	48	153	0.1435E+00	0.2198E-02	55998
slabs.xz30.sar	48	152	0.1527E+00	0.2248E-02	55998
slabs.xz31.sar	48	151	0.1625E+00	0.2297E-02	55998
slabs.xz32.sar	48	151	0.1728E+00	0.2348E-02	55998
slabs.xz33.sar	48	150	0.1838E+00	0.2402E-02	55998
slabs.xz34.sar	48	149	0.1952E+00	0.2459E-02	55998
slabs.xz35.sar	48	148	0.2072E+00	0.2522E-02	55998
slabs.xz36.sar	48	148	0.2197E+00	0.2591E-02	55998
slabs.xz37.sar	48	147	0.2328E+00	0.2665E-02	55998
slabs.xz38.sar	48	146	0.2462E+00	0.2747E-02	55998
slabs.xz39.sar	48	146	0.2600E+00	0.2835E-02	55998
slabs.xz40.sar	48	145	0.2742E+00	0.2931E-02	55998
slabs.xz41.sar	48	145	0.2885E+00	0.3033E-02	55998
slabs.xz42.sar	48	144	0.3031E+00	0.3141E-02	55998
slabs.xz43.sar	48	143	0.3176E+00	0.3255E-02	55998
slabs.xz44.sar	48	143	0.3324E+00	0.3375E-02	55998
slabs.xz45.sar	48	142	0.3468E+00	0.3500E-02	55998
slabs.xz46.sar	48	142	0.3614E+00	0.3630E-02	55998
slabs.xz47.sar	48	142	0.3756E+00	0.3763E-02	55998
slabs.xz48.sar	48	141	0.3896E+00	0.3901E-02	55998
slabs.xz49.sar	48	141	0.4033E+00	0.4042E-02	55998
slabs.xz50.sar	48	141	0.4166E+00	0.4186E-02	55998
slabs.xz51.sar	48	140	0.4297E+00	0.4332E-02	55998
slabs.xz52.sar	48	140	0.4423E+00	0.4481E-02	55998
slabs.xz53.sar	48	140	0.4545E+00	0.4632E-02	55998
slabs.xz54.sar	48	140	0.4663E+00	0.4784E-02	55998
slabs.xz55.sar	48	139	0.4777E+00	0.4937E-02	55998
slabs.xz56.sar	48	139	0.4889E+00	0.5090E-02	55998
slabs.xz57.sar	49	139	0.4999E+00	0.5243E-02	55998
slabs.xz58.sar	49	139	0.5109E+00	0.5394E-02	55998
slabs.xz59.sar	49	139	0.5215E+00	0.5543E-02	55998
slabs.xz60.sar	49	138	0.5319E+00	0.5690E-02	55998
slabs.xz61.sar	49	138	0.5421E+00	0.5832E-02	55998
slabs.xz62.sar	49	138	0.5520E+00	0.5970E-02	55998

Name of Slice Data File	Peak SAR x and z coordinates		Peak SAR (W/kg)	Avg. SAR (W/kg)	Voxels in tissue
slabs.xz63.sar	49	138	0.5616E+00	0.6103E-02	55998
slabs.xz64.sar	49	138	0.5708E+00	0.6230E-02	55998
slabs.xz65.sar	49	138	0.5798E+00	0.6350E-02	55998
slabs.xz66.sar	49	138	0.5884E+00	0.6463E-02	55998
slabs.xz67.sar	49	138	0.5966E+00	0.6568E-02	55998
slabs.xz68.sar	49	138	0.6044E+00	0.6669E-02	55998
slabs.xz69.sar	49	138	0.6118E+00	0.6715E-02	55998
slabs.xz70.sar	49	138	0.6187E+00	0.6802E-02	55998
slabs.xz71.sar	49	138	0.6251E+00	0.6884E-02	55998
slabs.xz72.sar	49	138	0.6310E+00	0.6961E-02	55998
slabs.xz73.sar	49	138	0.6363E+00	0.7034E-02	55998
slabs.xz74.sar	49	138	0.6410E+00	0.7102E-02	55998
slabs.xz75.sar	49	138	0.6450E+00	0.7165E-02	55998
slabs.xz76.sar	49	138	0.6485E+00	0.7223E-02	55998
slabs.xz77.sar	49	138	0.6513E+00	0.7276E-02	55998
slabs.xz78.sar	49	139	0.6534E+00	0.7323E-02	55998
slabs.xz79.sar	49	139	0.6551E+00	0.7364E-02	55998
slabs.xz80.sar	49	139	0.6561E+00	0.7399E-02	55998
slabs.xz81.sar	49	139	0.6565E+00	0.7427E-02	55998
slabs.xz82.sar	49	139	0.6563E+00	0.7450E-02	55998
slabs.xz83.sar	49	140	0.6556E+00	0.7512E-02	55998
slabs.xz84.sar	49	140	0.6544E+00	0.7516E-02	55998
slabs.xz85.sar	49	140	0.6527E+00	0.7509E-02	55998
slabs.xz86.sar	49	140	0.6503E+00	0.7490E-02	55998
slabs.xz87.sar	49	140	0.6475E+00	0.7457E-02	55998
slabs.xz88.sar	49	141	0.6442E+00	0.7413E-02	55998
slabs.xz89.sar	49	141	0.6404E+00	0.7355E-02	55998
slabs.xz90.sar	49	141	0.6361E+00	0.7286E-02	55998
slabs.xz91.sar	49	141	0.6311E+00	0.7204E-02	55998
slabs.xz92.sar	49	141	0.6255E+00	0.7111E-02	55998
slabs.xz93.sar	49	141	0.6193E+00	0.7007E-02	55998
slabs.xz94.sar	49	142	0.6125E+00	0.6893E-02	55998
slabs.xz95.sar	48	142	0.6056E+00	0.6770E-02	55998
slabs.xz96.sar	48	142	0.5981E+00	0.6638E-02	55998
slabs.xz97.sar	48	142	0.5898E+00	0.6498E-02	55998
slabs.xz98.sar	48	142	0.5806E+00	0.6351E-02	55998
slabs.xz99.sar	48	142	0.5704E+00	0.6198E-02	55998
slabs.xz100.sar	48	142	0.5593E+00	0.6038E-02	55998
slabs.xz101.sar	48	142	0.5472E+00	0.5874E-02	55998
slabs.xz102.sar	48	142	0.5341E+00	0.5706E-02	55998
slabs.xz103.sar	48	142	0.5201E+00	0.5533E-02	55998
slabs.xz104.sar	48	142	0.5050E+00	0.5358E-02	55998
slabs.xz105.sar	48	142	0.4889E+00	0.5181E-02	55998
slabs.xz106.sar	48	142	0.4719E+00	0.5002E-02	55998
slabs.xz107.sar	48	142	0.4541E+00	0.4822E-02	55998
slabs.xz108.sar	48	142	0.4354E+00	0.4642E-02	55998
slabs.xz109.sar	48	142	0.4160E+00	0.4462E-02	55998
slabs.xz110.sar	48	142	0.3960E+00	0.4284E-02	55998
slabs.xz111.sar	48	142	0.3755E+00	0.4107E-02	55998
slabs.xz112.sar	48	142	0.3547E+00	0.3933E-02	55998
slabs.xz113.sar	48	142	0.3336E+00	0.3763E-02	55998
slabs.xz114.sar	48	142	0.3123E+00	0.3597E-02	55998
slabs.xz115.sar	48	142	0.2911E+00	0.3436E-02	55998
slabs.xz116.sar	48	142	0.2701E+00	0.3280E-02	55998
slabs.xz117.sar	48	142	0.2493E+00	0.3131E-02	55998

Name of Slice Data File	Peak SAR x and z coordinates		Peak SAR (W/kg)	Avg. SAR (W/kg)	Voxels in tissue
slabs.xz118.sar	48	141	0.2291E+00	0.2989E-02	55998
slabs.xz119.sar	48	141	0.2093E+00	0.2854E-02	55998
slabs.xz120.sar	48	141	0.1903E+00	0.2728E-02	55998
slabs.xz121.sar	48	141	0.1720E+00	0.2609E-02	55998
slabs.xz122.sar	48	141	0.1546E+00	0.2499E-02	55998
slabs.xz123.sar	49	141	0.1384E+00	0.2399E-02	55998
slabs.xz124.sar	49	141	0.1231E+00	0.2307E-02	55998
slabs.xz125.sar	48	63	0.1173E+00	0.2224E-02	55998
slabs.xz126.sar	49	64	0.1148E+00	0.2151E-02	55998
slabs.xz127.sar	49	64	0.1124E+00	0.2087E-02	55998
slabs.xz128.sar	48	211	0.1191E+00	0.2032E-02	55998
slabs.xz129.sar	48	211	0.1295E+00	0.1985E-02	55998
slabs.xz130.sar	48	211	0.1403E+00	0.1948E-02	55998
slabs.xz131.sar	48	211	0.1512E+00	0.1919E-02	55998
slabs.xz132.sar	48	211	0.1624E+00	0.1898E-02	55998
slabs.xz133.sar	48	211	0.1737E+00	0.1885E-02	55998
slabs.xz134.sar	48	211	0.1850E+00	0.1879E-02	55998
slabs.xz135.sar	48	211	0.1963E+00	0.1880E-02	55998
slabs.xz136.sar	48	211	0.2074E+00	0.1888E-02	55998
slabs.xz137.sar	48	212	0.2185E+00	0.1901E-02	55998
slabs.xz138.sar	48	212	0.2294E+00	0.1920E-02	55998
slabs.xz139.sar	48	212	0.2399E+00	0.1943E-02	55998
slabs.xz140.sar	48	212	0.2500E+00	0.1970E-02	55998
slabs.xz141.sar	48	212	0.2596E+00	0.2001E-02	55998
slabs.xz142.sar	48	212	0.2687E+00	0.2034E-02	55998
slabs.xz143.sar	48	212	0.2770E+00	0.2069E-02	55998
slabs.xz144.sar	48	212	0.2847E+00	0.2104E-02	55998
slabs.xz145.sar	48	213	0.2917E+00	0.2140E-02	55998
slabs.xz146.sar	48	213	0.2979E+00	0.2176E-02	55998
slabs.xz147.sar	48	213	0.3032E+00	0.2210E-02	55998
slabs.xz148.sar	48	213	0.3075E+00	0.2242E-02	55998
slabs.xz149.sar	48	213	0.3108E+00	0.2271E-02	55998
slabs.xz150.sar	48	213	0.3131E+00	0.2297E-02	55998
slabs.xz151.sar	48	214	0.3146E+00	0.2319E-02	55998
slabs.xz152.sar	48	214	0.3151E+00	0.2337E-02	55998
slabs.xz153.sar	48	214	0.3145E+00	0.2351E-02	55998
slabs.xz154.sar	48	214	0.3128E+00	0.2359E-02	55998
slabs.xz155.sar	48	215	0.3102E+00	0.2363E-02	55998
slabs.xz156.sar	48	215	0.3068E+00	0.2361E-02	55998
slabs.xz157.sar	48	215	0.3023E+00	0.2355E-02	55998
slabs.xz158.sar	48	215	0.2969E+00	0.2344E-02	55998
slabs.xz159.sar	48	216	0.2910E+00	0.2328E-02	55998
slabs.xz160.sar	48	216	0.2842E+00	0.2308E-02	55998
slabs.xz161.sar	48	216	0.2766E+00	0.2284E-02	55998
slabs.xz162.sar	48	217	0.2687E+00	0.2257E-02	55998
slabs.xz163.sar	48	217	0.2602E+00	0.2227E-02	55998
slabs.xz164.sar	48	218	0.2513E+00	0.2196E-02	55998
slabs.xz165.sar	48	218	0.2421E+00	0.2163E-02	55998
slabs.xz166.sar	48	219	0.2326E+00	0.2130E-02	55998
slabs.xz167.sar	48	219	0.2230E+00	0.2097E-02	55998
slabs.xz168.sar	48	220	0.2134E+00	0.2064E-02	55998
slabs.xz169.sar	48	220	0.2038E+00	0.2034E-02	55998
slabs.xz170.sar	48	221	0.1944E+00	0.2006E-02	55998
slabs.xz171.sar	48	222	0.1851E+00	0.1982E-02	55998
slabs.xz172.sar	49	222	0.1762E+00	0.1961E-02	55998

Name of Slice Data File	Peak SAR x and z coordinates		Peak SAR (W/kg)	Avg. SAR (W/kg)	Voxels in tissue
slabs.xz173.sar	49	223	0.1678E+00	0.1945E-02	55998
slabs.xz174.sar	49	224	0.1596E+00	0.1934E-02	55998
slabs.xz175.sar	49	225	0.1518E+00	0.1930E-02	55998
slabs.xz176.sar	49	226	0.1444E+00	0.1932E-02	55998
slabs.xz177.sar	49	226	0.1375E+00	0.1941E-02	55998
slabs.xz178.sar	49	227	0.1311E+00	0.1957E-02	55998
slabs.xz179.sar	48	59	0.1268E+00	0.1982E-02	55998
slabs.xz180.sar	48	59	0.1300E+00	0.2015E-02	55998
slabs.xz181.sar	48	59	0.1331E+00	0.2057E-02	55998
slabs.xz182.sar	48	59	0.1360E+00	0.2109E-02	55998
slabs.xz183.sar	48	59	0.1388E+00	0.2170E-02	55998
slabs.xz184.sar	48	59	0.1414E+00	0.2241E-02	55998
slabs.xz185.sar	48	59	0.1437E+00	0.2321E-02	55998
slabs.xz186.sar	48	59	0.1458E+00	0.2411E-02	55998
slabs.xz187.sar	49	140	0.1558E+00	0.2512E-02	55998
slabs.xz188.sar	49	140	0.1738E+00	0.2622E-02	55998
slabs.xz189.sar	49	140	0.1928E+00	0.2741E-02	55998
slabs.xz190.sar	49	140	0.2127E+00	0.2870E-02	55998
slabs.xz191.sar	49	140	0.2334E+00	0.3008E-02	55998
slabs.xz192.sar	49	140	0.2549E+00	0.3155E-02	55998
slabs.xz193.sar	49	140	0.2770E+00	0.3310E-02	55998
slabs.xz194.sar	49	140	0.2996E+00	0.3472E-02	55998
slabs.xz195.sar	49	140	0.3227E+00	0.3641E-02	55998
slabs.xz196.sar	49	140	0.3460E+00	0.3816E-02	55998
slabs.xz197.sar	49	140	0.3695E+00	0.3996E-02	55998
slabs.xz198.sar	49	140	0.3930E+00	0.4182E-02	55998
slabs.xz199.sar	48	140	0.4167E+00	0.4371E-02	55998
slabs.xz200.sar	48	140	0.4401E+00	0.4563E-02	55998
slabs.xz201.sar	48	140	0.4632E+00	0.4757E-02	55998
slabs.xz202.sar	48	140	0.4858E+00	0.4953E-02	55998
slabs.xz203.sar	48	140	0.5079E+00	0.5149E-02	55998
slabs.xz204.sar	48	140	0.5294E+00	0.5345E-02	55998
slabs.xz205.sar	49	141	0.5503E+00	0.5541E-02	55998
slabs.xz206.sar	49	141	0.5705E+00	0.5734E-02	55998
slabs.xz207.sar	49	141	0.5900E+00	0.5925E-02	55998
slabs.xz208.sar	49	141	0.6087E+00	0.6112E-02	55998
slabs.xz209.sar	49	141	0.6265E+00	0.6296E-02	55998
slabs.xz210.sar	49	141	0.6435E+00	0.6475E-02	55998
slabs.xz211.sar	49	141	0.6595E+00	0.6648E-02	55998
slabs.xz212.sar	49	140	0.6747E+00	0.6815E-02	55998
slabs.xz213.sar	49	140	0.6889E+00	0.6976E-02	55998
slabs.xz214.sar	49	140	0.7023E+00	0.7130E-02	55998
slabs.xz215.sar	49	140	0.7147E+00	0.7276E-02	55998
slabs.xz216.sar	49	140	0.7262E+00	0.7413E-02	55998
slabs.xz217.sar	49	140	0.7369E+00	0.7542E-02	55998
slabs.xz218.sar	49	140	0.7467E+00	0.7661E-02	55998
slabs.xz219.sar	49	140	0.7556E+00	0.7771E-02	55998
slabs.xz220.sar	49	140	0.7637E+00	0.7870E-02	55998
slabs.xz221.sar	49	140	0.7711E+00	0.7959E-02	55998
slabs.xz222.sar	49	140	0.7776E+00	0.8036E-02	55998
slabs.xz223.sar	49	140	0.7834E+00	0.8103E-02	55998
slabs.xz224.sar	49	140	0.7884E+00	0.8158E-02	55998
slabs.xz225.sar	49	140	0.7928E+00	0.8201E-02	55998
slabs.xz226.sar	49	140	0.7964E+00	0.8233E-02	55998
slabs.xz227.sar	49	140	0.7994E+00	0.8253E-02	55998

Name of Slice Data File	Peak SAR x and z coordinates		Peak SAR (W/kg)	Avg. SAR (W/kg)	Voxels in tissue
slabs.xz228.sar	49	140	0.8018E+00	0.8261E-02	55998
slabs.xz229.sar	49	140	0.8034E+00	0.8256E-02	55998
slabs.xz230.sar	49	139	0.8046E+00	0.8241E-02	55998
slabs.xz231.sar	49	139	0.8051E+00	0.8213E-02	55998
slabs.xz232.sar	49	139	0.8050E+00	0.8174E-02	55998
slabs.xz233.sar	49	139	0.8042E+00	0.8123E-02	55998
slabs.xz234.sar	49	139	0.8028E+00	0.8061E-02	55998
slabs.xz235.sar	49	139	0.8008E+00	0.7989E-02	55998
slabs.xz236.sar	49	139	0.7982E+00	0.7906E-02	55998
slabs.xz237.sar	49	139	0.7948E+00	0.7813E-02	55998
slabs.xz238.sar	49	139	0.7909E+00	0.7710E-02	55998
slabs.xz239.sar	49	139	0.7862E+00	0.7598E-02	55998
slabs.xz240.sar	49	139	0.7809E+00	0.7477E-02	55998
slabs.xz241.sar	48	139	0.7751E+00	0.7348E-02	55998
slabs.xz242.sar	48	139	0.7690E+00	0.7212E-02	55998
slabs.xz243.sar	48	139	0.7622E+00	0.7069E-02	55998
slabs.xz244.sar	48	139	0.7547E+00	0.6920E-02	55998
slabs.xz245.sar	48	139	0.7465E+00	0.6765E-02	55998
slabs.xz246.sar	48	139	0.7374E+00	0.6606E-02	55998
slabs.xz247.sar	48	138	0.7276E+00	0.6443E-02	55998
slabs.xz248.sar	48	138	0.7171E+00	0.6276E-02	55998
slabs.xz249.sar	48	138	0.7057E+00	0.6108E-02	55998
slabs.xz250.sar	48	138	0.6936E+00	0.5937E-02	55998
slabs.xz251.sar	48	138	0.6806E+00	0.5766E-02	55998
slabs.xz252.sar	48	138	0.6669E+00	0.5594E-02	55998
slabs.xz253.sar	48	138	0.6525E+00	0.5422E-02	55998
slabs.xz254.sar	48	138	0.6372E+00	0.5251E-02	55998
slabs.xz255.sar	48	138	0.6213E+00	0.5082E-02	55998
slabs.xz256.sar	48	138	0.6047E+00	0.4914E-02	55998
slabs.xz257.sar	48	138	0.5875E+00	0.4748E-02	55998
slabs.xz258.sar	48	139	0.5696E+00	0.4584E-02	55998
slabs.xz259.sar	48	139	0.5513E+00	0.4424E-02	55998
slabs.xz260.sar	48	139	0.5325E+00	0.4267E-02	55998
slabs.xz261.sar	48	139	0.5132E+00	0.4113E-02	55998
slabs.xz262.sar	48	139	0.4936E+00	0.3963E-02	55998
slabs.xz263.sar	48	139	0.4736E+00	0.3819E-02	55998
slabs.xz264.sar	48	139	0.4534E+00	0.3679E-02	55998
slabs.xz265.sar	48	139	0.4329E+00	0.3545E-02	55998
slabs.xz266.sar	48	139	0.4124E+00	0.3418E-02	55998
slabs.xz267.sar	48	139	0.3918E+00	0.3297E-02	55998
slabs.xz268.sar	48	139	0.3713E+00	0.3184E-02	55998
slabs.xz269.sar	48	140	0.3509E+00	0.3078E-02	55998
slabs.xz270.sar	48	140	0.3309E+00	0.2981E-02	55998
slabs.xz271.sar	48	140	0.3112E+00	0.2892E-02	55998
slabs.xz272.sar	48	140	0.2919E+00	0.2811E-02	55998
slabs.xz273.sar	48	140	0.2730E+00	0.2738E-02	55998
slabs.xz274.sar	48	140	0.2547E+00	0.2671E-02	55998
slabs.xz275.sar	48	141	0.2371E+00	0.2611E-02	55998
slabs.xz276.sar	48	141	0.2203E+00	0.2556E-02	55998
slabs.xz277.sar	48	141	0.2042E+00	0.2503E-02	55998
slabs.xz278.sar	48	141	0.1889E+00	0.2452E-02	55998
slabs.xz279.sar	48	141	0.1743E+00	0.2400E-02	55998
slabs.xz280.sar	48	142	0.1606E+00	0.2345E-02	55998
slabs.xz281.sar	48	226	0.1569E+00	0.2285E-02	55998
slabs.xz282.sar	48	226	0.1602E+00	0.2218E-02	55998

Name of Slice Data File	Peak SAR x and z coordinates		Peak SAR (W/kg)	Avg. SAR (W/kg)	Voxels in tissue
slabs.xz283.sar	48	225	0.1620E+00	0.2142E-02	55998
slabs.xz284.sar	48	225	0.1623E+00	0.2055E-02	55998
slabs.xz285.sar	48	225	0.1606E+00	0.1957E-02	55998
slabs.xz286.sar	48	225	0.1570E+00	0.1847E-02	55998
slabs.xz287.sar	48	225	0.1513E+00	0.1726E-02	55998
slabs.xz288.sar	48	225	0.1435E+00	0.1595E-02	55998
slabs.xz289.sar	48	225	0.1335E+00	0.1454E-02	55998
slabs.xz290.sar	48	230	0.1281E+00	0.1241E-02	55998
slabs.xz291.sar	48	225	0.1089E+00	0.1163E-02	55998
slabs.xz292.sar	48	225	0.9378E-01	0.1006E-02	55997

Location and values for peak and average SAR for total volume of exposed tissue

slabs.xz231.sar	49	139	0.8051E+00	0.4233E-02	15567443

Table 8.2. Slice and Whole Slab Model Peak and average (averaged over slice) 1 Gram Average SAR for Inhomogeneous Slab Model Exposed to AT&T RU Antenna with Outside Skin Surface in Contact with Radome Centered at Middle of Patch Array (xz-plane slice file number is distance in mm from FDTD space rectangular coordinates origin in y direction).

Name of Slice Data File	Peak SAR x and z coordinates		Peak SAR (W/kg)	Avg. SAR (W/kg)	Voxels in tissue
slabs.xz15.1gsar	48	239	0.2470E-01	0.1068E-02	55998
slabs.xz16.1gsar	48	161	0.2598E-01	0.1083E-02	55998
slabs.xz17.1gsar	48	161	0.2598E-01	0.1107E-02	55998
slabs.xz18.1gsar	48	161	0.3080E-01	0.1116E-02	55998
slabs.xz19.1gsar	48	160	0.3238E-01	0.1258E-02	55998
slabs.xz20.1gsar	48	160	0.3398E-01	0.1223E-02	55998
slabs.xz21.1gsar	48	159	0.3558E-01	0.1316E-02	55998
slabs.xz22.1gsar	48	159	0.3865E-01	0.1408E-02	55998
slabs.xz23.1gsar	48	158	0.4178E-01	0.1494E-02	55998
slabs.xz24.1gsar	48	157	0.4496E-01	0.1572E-02	55998
slabs.xz25.1gsar	48	157	0.4821E-01	0.1645E-02	55998
slabs.xz26.1gsar	48	156	0.5160E-01	0.1710E-02	55998
slabs.xz27.1gsar	48	155	0.5512E-01	0.1770E-02	55998
slabs.xz28.1gsar	48	154	0.5878E-01	0.1826E-02	55998
slabs.xz29.1gsar	48	154	0.6264E-01	0.1877E-02	55998
slabs.xz30.1gsar	48	153	0.6670E-01	0.1926E-02	55998
slabs.xz31.1gsar	48	152	0.7095E-01	0.1974E-02	55998
slabs.xz32.1gsar	48	151	0.7540E-01	0.2022E-02	55998
slabs.xz33.1gsar	48	151	0.8010E-01	0.2072E-02	55998
slabs.xz34.1gsar	48	150	0.8501E-01	0.2124E-02	55998
slabs.xz35.1gsar	48	149	0.9012E-01	0.2179E-02	55998
slabs.xz36.1gsar	48	149	0.9543E-01	0.2238E-02	55998
slabs.xz37.1gsar	48	148	0.1010E+00	0.2302E-02	55998
slabs.xz38.1gsar	48	147	0.1066E+00	0.2370E-02	55998
slabs.xz39.1gsar	48	147	0.1124E+00	0.2444E-02	55998
slabs.xz40.1gsar	48	146	0.1184E+00	0.2523E-02	55998
slabs.xz41.1gsar	48	146	0.1244E+00	0.2608E-02	55998
slabs.xz42.1gsar	48	145	0.1306E+00	0.2697E-02	55998
slabs.xz43.1gsar	48	144	0.1367E+00	0.2791E-02	55998
slabs.xz44.1gsar	48	144	0.1430E+00	0.2891E-02	55998
slabs.xz45.1gsar	48	144	0.1491E+00	0.2994E-02	55998
slabs.xz46.1gsar	48	143	0.1553E+00	0.3101E-02	55998
slabs.xz47.1gsar	48	143	0.1614E+00	0.3212E-02	55998
slabs.xz48.1gsar	48	142	0.1673E+00	0.3327E-02	55998
slabs.xz49.1gsar	48	142	0.1733E+00	0.3444E-02	55998
slabs.xz50.1gsar	48	142	0.1790E+00	0.3565E-02	55998
slabs.xz51.1gsar	48	141	0.1847E+00	0.3687E-02	55998
slabs.xz52.1gsar	48	141	0.1902E+00	0.3811E-02	55998
slabs.xz53.1gsar	48	141	0.1956E+00	0.3937E-02	55998
slabs.xz54.1gsar	48	141	0.2008E+00	0.4064E-02	55998
slabs.xz55.1gsar	48	140	0.2059E+00	0.4191E-02	55998
slabs.xz56.1gsar	48	140	0.2108E+00	0.4319E-02	55998
slabs.xz57.1gsar	48	140	0.2156E+00	0.4445E-02	55998
slabs.xz58.1gsar	48	140	0.2202E+00	0.4571E-02	55998
slabs.xz59.1gsar	48	140	0.2247E+00	0.4694E-02	55998
slabs.xz60.1gsar	48	140	0.2290E+00	0.4815E-02	55998
slabs.xz61.1gsar	48	139	0.2332E+00	0.4933E-02	55998
slabs.xz62.1gsar	48	139	0.2373E+00	0.5046E-02	55998

Name of Slice Data File	Peak SAR x and z coordinates		Peak SAR (W/kg)	Avg. SAR (W/kg)	Voxels in tissue
slabs.xz63.1gsar	48	139	0.2412E+00	0.5156E-02	55998
slabs.xz64.1gsar	48	139	0.2450E+00	0.5256E-02	55998
slabs.xz65.1gsar	48	139	0.2486E+00	0.5352E-02	55998
slabs.xz66.1gsar	48	139	0.2520E+00	0.5442E-02	55998
slabs.xz67.1gsar	48	139	0.2553E+00	0.5527E-02	55998
slabs.xz68.1gsar	48	139	0.2585E+00	0.5607E-02	55998
slabs.xz69.1gsar	48	139	0.2614E+00	0.5682E-02	55998
slabs.xz70.1gsar	48	139	0.2642E+00	0.5753E-02	55998
slabs.xz71.1gsar	48	139	0.2667E+00	0.5818E-02	55998
slabs.xz72.1gsar	48	139	0.2691E+00	0.5879E-02	55998
slabs.xz73.1gsar	48	139	0.2712E+00	0.5936E-02	55998
slabs.xz74.1gsar	48	139	0.2731E+00	0.5989E-02	55998
slabs.xz75.1gsar	48	139	0.2748E+00	0.6041E-02	55998
slabs.xz76.1gsar	48	139	0.2762E+00	0.6090E-02	55998
slabs.xz77.1gsar	48	140	0.2775E+00	0.6134E-02	55998
slabs.xz78.1gsar	48	140	0.2785E+00	0.6179E-02	55998
slabs.xz79.1gsar	48	140	0.2793E+00	0.6218E-02	55998
slabs.xz80.1gsar	48	140	0.2798E+00	0.6252E-02	55998
slabs.xz81.1gsar	48	140	0.2801E+00	0.6279E-02	55998
slabs.xz82.1gsar	48	141	0.2802E+00	0.6300E-02	55998
slabs.xz83.1gsar	48	141	0.2801E+00	0.6313E-02	55998
slabs.xz84.1gsar	48	141	0.2798E+00	0.6317E-02	55998
slabs.xz85.1gsar	48	141	0.2793E+00	0.6314E-02	55998
slabs.xz86.1gsar	48	141	0.2785E+00	0.6300E-02	55998
slabs.xz87.1gsar	48	142	0.2775E+00	0.6277E-02	55998
slabs.xz88.1gsar	48	142	0.2763E+00	0.6244E-02	55998
slabs.xz89.1gsar	48	142	0.2749E+00	0.6196E-02	55998
slabs.xz90.1gsar	48	142	0.2732E+00	0.6138E-02	55998
slabs.xz91.1gsar	48	142	0.2713E+00	0.6070E-02	55998
slabs.xz92.1gsar	48	142	0.2690E+00	0.5992E-02	55998
slabs.xz93.1gsar	48	142	0.2665E+00	0.5905E-02	55998
slabs.xz94.1gsar	48	143	0.2637E+00	0.5810E-02	55998
slabs.xz95.1gsar	48	143	0.2606E+00	0.5706E-02	55998
slabs.xz96.1gsar	48	143	0.2571E+00	0.5596E-02	55998
slabs.xz97.1gsar	48	143	0.2533E+00	0.5478E-02	55998
slabs.xz98.1gsar	48	143	0.2491E+00	0.5355E-02	55998
slabs.xz99.1gsar	48	143	0.2446E+00	0.5226E-02	55998
slabs.xz100.1gsar	48	143	0.2396E+00	0.5092E-02	55998
slabs.xz101.1gsar	48	143	0.2343E+00	0.4955E-02	55998
slabs.xz102.1gsar	48	143	0.2285E+00	0.4814E-02	55998
slabs.xz103.1gsar	48	143	0.2224E+00	0.4671E-02	55998
slabs.xz104.1gsar	48	143	0.2159E+00	0.4525E-02	55998
slabs.xz105.1gsar	48	143	0.2090E+00	0.4378E-02	55998
slabs.xz106.1gsar	48	143	0.2018E+00	0.4230E-02	55998
slabs.xz107.1gsar	48	143	0.1942E+00	0.4081E-02	55998
slabs.xz108.1gsar	48	143	0.1864E+00	0.3933E-02	55998
slabs.xz109.1gsar	48	143	0.1783E+00	0.3786E-02	55998
slabs.xz110.1gsar	48	143	0.1699E+00	0.3639E-02	55998
slabs.xz111.1gsar	48	143	0.1614E+00	0.3495E-02	55998
slabs.xz112.1gsar	48	143	0.1527E+00	0.3353E-02	55998
slabs.xz113.1gsar	48	143	0.1440E+00	0.3214E-02	55998
slabs.xz114.1gsar	48	143	0.1352E+00	0.3079E-02	55998
slabs.xz115.1gsar	48	142	0.1265E+00	0.2948E-02	55998
slabs.xz116.1gsar	48	142	0.1178E+00	0.2821E-02	55998
slabs.xz117.1gsar	48	142	0.1092E+00	0.2700E-02	55998

Name of Slice Data File	Peak SAR x and z coordinates		Peak SAR (W/kg)	Avg. SAR (W/kg)	Voxels in tissue
slabs.xz118.1gsar	48	142	0.1008E+00	0.2584E-02	55998
slabs.xz119.1gsar	48	142	0.9263E-01	0.2474E-02	55998
slabs.xz120.1gsar	48	142	0.8470E-01	0.2370E-02	55998
slabs.xz121.1gsar	48	142	0.7707E-01	0.2273E-02	55998
slabs.xz122.1gsar	48	142	0.6976E-01	0.2183E-02	55998
slabs.xz123.1gsar	48	142	0.6281E-01	0.2099E-02	55998
slabs.xz124.1gsar	48	142	0.5624E-01	0.2023E-02	55998
slabs.xz125.1gsar	48	64	0.5147E-01	0.1955E-02	55998
slabs.xz126.1gsar	48	64	0.5045E-01	0.1893E-02	55998
slabs.xz127.1gsar	48	64	0.4943E-01	0.1839E-02	55998
slabs.xz128.1gsar	48	212	0.5291E-01	0.1792E-02	55998
slabs.xz129.1gsar	48	212	0.5716E-01	0.1752E-02	55998
slabs.xz130.1gsar	48	212	0.6152E-01	0.1720E-02	55998
slabs.xz131.1gsar	48	213	0.6597E-01	0.1694E-02	55998
slabs.xz132.1gsar	48	213	0.7050E-01	0.1674E-02	55998
slabs.xz133.1gsar	48	213	0.7507E-01	0.1661E-02	55998
slabs.xz134.1gsar	48	213	0.7965E-01	0.1654E-02	55998
slabs.xz135.1gsar	48	213	0.8422E-01	0.1652E-02	55998
slabs.xz136.1gsar	48	213	0.8874E-01	0.1656E-02	55998
slabs.xz137.1gsar	48	213	0.9319E-01	0.1664E-02	55998
slabs.xz138.1gsar	48	213	0.9753E-01	0.1677E-02	55998
slabs.xz139.1gsar	48	213	0.1017E+00	0.1693E-02	55998
slabs.xz140.1gsar	48	213	0.1058E+00	0.1713E-02	55998
slabs.xz141.1gsar	48	213	0.1096E+00	0.1735E-02	55998
slabs.xz142.1gsar	48	213	0.1132E+00	0.1759E-02	55998
slabs.xz143.1gsar	48	214	0.1165E+00	0.1785E-02	55998
slabs.xz144.1gsar	48	214	0.1196E+00	0.1811E-02	55998
slabs.xz145.1gsar	48	214	0.1224E+00	0.1838E-02	55998
slabs.xz146.1gsar	48	214	0.1249E+00	0.1864E-02	55998
slabs.xz147.1gsar	48	214	0.1270E+00	0.1889E-02	55998
slabs.xz148.1gsar	48	214	0.1287E+00	0.1913E-02	55998
slabs.xz149.1gsar	48	214	0.1301E+00	0.1935E-02	55998
slabs.xz150.1gsar	48	215	0.1311E+00	0.1954E-02	55998
slabs.xz151.1gsar	48	215	0.1317E+00	0.1970E-02	55998
slabs.xz152.1gsar	48	215	0.1319E+00	0.1984E-02	55998
slabs.xz153.1gsar	48	215	0.1316E+00	0.1993E-02	55998
slabs.xz154.1gsar	48	215	0.1310E+00	0.1999E-02	55998
slabs.xz155.1gsar	48	216	0.1300E+00	0.2002E-02	55998
slabs.xz156.1gsar	48	216	0.1287E+00	0.2000E-02	55998
slabs.xz157.1gsar	48	216	0.1270E+00	0.1995E-02	55998
slabs.xz158.1gsar	48	216	0.1249E+00	0.1986E-02	55998
slabs.xz159.1gsar	48	217	0.1225E+00	0.1973E-02	55998
slabs.xz160.1gsar	48	217	0.1199E+00	0.1958E-02	55998
slabs.xz161.1gsar	48	217	0.1169E+00	0.1939E-02	55998
slabs.xz162.1gsar	48	218	0.1137E+00	0.1918E-02	55998
slabs.xz163.1gsar	48	218	0.1103E+00	0.1896E-02	55998
slabs.xz164.1gsar	48	218	0.1067E+00	0.1871E-02	55998
slabs.xz165.1gsar	48	219	0.1031E+00	0.1846E-02	55998
slabs.xz166.1gsar	48	219	0.9923E-01	0.1821E-02	55998
slabs.xz167.1gsar	48	220	0.9534E-01	0.1796E-02	55998
slabs.xz168.1gsar	48	220	0.9141E-01	0.1772E-02	55998
slabs.xz169.1gsar	48	221	0.8749E-01	0.1749E-02	55998
slabs.xz170.1gsar	48	222	0.8356E-01	0.1728E-02	55998
slabs.xz171.1gsar	48	222	0.7974E-01	0.1710E-02	55998
slabs.xz172.1gsar	48	223	0.7599E-01	0.1695E-02	55998

Name of Slice Data File	Peak SAR x and z coordinates		Peak SAR (W/kg)	Avg. SAR (W/kg)	Voxels in tissue
slabs.xz173.1gsar	48	224	0.7234E-01	0.1684E-02	55998
slabs.xz174.1gsar	48	224	0.6883E-01	0.1678E-02	55998
slabs.xz175.1gsar	48	225	0.6551E-01	0.1676E-02	55998
slabs.xz176.1gsar	48	226	0.6235E-01	0.1680E-02	55998
slabs.xz177.1gsar	48	227	0.5937E-01	0.1690E-02	55998
slabs.xz178.1gsar	48	228	0.5658E-01	0.1706E-02	55998
slabs.xz179.1gsar	48	60	0.5485E-01	0.1728E-02	55998
slabs.xz180.1gsar	48	60	0.5604E-01	0.1757E-02	55998
slabs.xz181.1gsar	48	60	0.5718E-01	0.1794E-02	55998
slabs.xz182.1gsar	48	60	0.5827E-01	0.1838E-02	55998
slabs.xz183.1gsar	48	60	0.5928E-01	0.1890E-02	55998
slabs.xz184.1gsar	48	60	0.6023E-01	0.1949E-02	55998
slabs.xz185.1gsar	48	60	0.6108E-01	0.2017E-02	55998
slabs.xz186.1gsar	48	141	0.6248E-01	0.2092E-02	55998
slabs.xz187.1gsar	48	141	0.6972E-01	0.2175E-02	55998
slabs.xz188.1gsar	48	141	0.7740E-01	0.2266E-02	55998
slabs.xz189.1gsar	48	141	0.8548E-01	0.2365E-02	55998
slabs.xz190.1gsar	48	141	0.9393E-01	0.2471E-02	55998
slabs.xz191.1gsar	48	141	0.1027E+00	0.2585E-02	55998
slabs.xz192.1gsar	48	141	0.1118E+00	0.2705E-02	55998
slabs.xz193.1gsar	48	141	0.1212E+00	0.2832E-02	55998
slabs.xz194.1gsar	48	141	0.1307E+00	0.2965E-02	55998
slabs.xz195.1gsar	48	141	0.1405E+00	0.3103E-02	55998
slabs.xz196.1gsar	48	141	0.1503E+00	0.3247E-02	55998
slabs.xz197.1gsar	48	141	0.1603E+00	0.3395E-02	55998
slabs.xz198.1gsar	48	141	0.1702E+00	0.3547E-02	55998
slabs.xz199.1gsar	48	141	0.1801E+00	0.3702E-02	55998
slabs.xz200.1gsar	48	141	0.1900E+00	0.3860E-02	55998
slabs.xz201.1gsar	48	141	0.1997E+00	0.4021E-02	55998
slabs.xz202.1gsar	48	141	0.2093E+00	0.4182E-02	55998
slabs.xz203.1gsar	48	141	0.2186E+00	0.4345E-02	55998
slabs.xz204.1gsar	48	141	0.2278E+00	0.4507E-02	55998
slabs.xz205.1gsar	48	141	0.2367E+00	0.4669E-02	55998
slabs.xz206.1gsar	48	141	0.2452E+00	0.4830E-02	55998
slabs.xz207.1gsar	48	141	0.2535E+00	0.4989E-02	55998
slabs.xz208.1gsar	48	141	0.2614E+00	0.5146E-02	55998
slabs.xz209.1gsar	48	141	0.2690E+00	0.5299E-02	55998
slabs.xz210.1gsar	48	141	0.2762E+00	0.5449E-02	55998
slabs.xz211.1gsar	48	141	0.2831E+00	0.5595E-02	55998
slabs.xz212.1gsar	48	141	0.2895E+00	0.5736E-02	55998
slabs.xz213.1gsar	48	141	0.2956E+00	0.5872E-02	55998
slabs.xz214.1gsar	48	141	0.3013E+00	0.6001E-02	55998
slabs.xz215.1gsar	48	141	0.3066E+00	0.6124E-02	55998
slabs.xz216.1gsar	48	141	0.3116E+00	0.6241E-02	55998
slabs.xz217.1gsar	48	141	0.3162E+00	0.6350E-02	55998
slabs.xz218.1gsar	48	141	0.3204E+00	0.6451E-02	55998
slabs.xz219.1gsar	48	141	0.3242E+00	0.6544E-02	55998
slabs.xz220.1gsar	48	141	0.3277E+00	0.6628E-02	55998
slabs.xz221.1gsar	48	141	0.3309E+00	0.6704E-02	55998
slabs.xz222.1gsar	48	141	0.3338E+00	0.6770E-02	55998
slabs.xz223.1gsar	48	141	0.3363E+00	0.6827E-02	55998
slabs.xz224.1gsar	48	141	0.3386E+00	0.6874E-02	55998
slabs.xz225.1gsar	48	141	0.3405E+00	0.6911E-02	55998
slabs.xz226.1gsar	48	141	0.3422E+00	0.6938E-02	55998
slabs.xz227.1gsar	48	141	0.3435E+00	0.6955E-02	55998

Name of Slice Data File	Peak SAR x and z coordinates		Peak SAR (W/kg)	Avg. SAR (W/kg)	Voxels in tissue
slabs.xz228.1gsar	48	141	0.3446E+00	0.6962E-02	55998
slabs.xz229.1gsar	48	141	0.3455E+00	0.6959E-02	55998
slabs.xz230.1gsar	48	140	0.3460E+00	0.6946E-02	55998
slabs.xz231.1gsar	48	140	0.3464E+00	0.6922E-02	55998
slabs.xz232.1gsar	48	140	0.3464E+00	0.6890E-02	55998
slabs.xz233.1gsar	48	140	0.3462E+00	0.6847E-02	55998
slabs.xz234.1gsar	48	140	0.3458E+00	0.6795E-02	55998
slabs.xz235.1gsar	48	140	0.3450E+00	0.6735E-02	55998
slabs.xz236.1gsar	48	140	0.3440E+00	0.6665E-02	55998
slabs.xz237.1gsar	48	140	0.3427E+00	0.6587E-02	55998
slabs.xz238.1gsar	48	140	0.3412E+00	0.6500E-02	55998
slabs.xz239.1gsar	48	140	0.3393E+00	0.6407E-02	55998
slabs.xz240.1gsar	48	140	0.3371E+00	0.6306E-02	55998
slabs.xz241.1gsar	48	140	0.3347E+00	0.6198E-02	55998
slabs.xz242.1gsar	48	140	0.3319E+00	0.6085E-02	55998
slabs.xz243.1gsar	48	140	0.3288E+00	0.5965E-02	55998
slabs.xz244.1gsar	48	140	0.3254E+00	0.5841E-02	55998
slabs.xz245.1gsar	48	140	0.3217E+00	0.5713E-02	55998
slabs.xz246.1gsar	48	140	0.3176E+00	0.5581E-02	55998
slabs.xz247.1gsar	48	140	0.3133E+00	0.5446E-02	55998
slabs.xz248.1gsar	48	140	0.3085E+00	0.5308E-02	55998
slabs.xz249.1gsar	48	139	0.3035E+00	0.5169E-02	55998
slabs.xz250.1gsar	48	139	0.2982E+00	0.5028E-02	55998
slabs.xz251.1gsar	48	139	0.2925E+00	0.4886E-02	55998
slabs.xz252.1gsar	48	139	0.2865E+00	0.4744E-02	55998
slabs.xz253.1gsar	48	139	0.2802E+00	0.4603E-02	55998
slabs.xz254.1gsar	48	139	0.2736E+00	0.4462E-02	55998
slabs.xz255.1gsar	48	140	0.2667E+00	0.4321E-02	55998
slabs.xz256.1gsar	48	140	0.2596E+00	0.4183E-02	55998
slabs.xz257.1gsar	48	140	0.2522E+00	0.4046E-02	55998
slabs.xz258.1gsar	48	140	0.2445E+00	0.3911E-02	55998
slabs.xz259.1gsar	48	140	0.2367E+00	0.3778E-02	55998
slabs.xz260.1gsar	48	140	0.2286E+00	0.3649E-02	55998
slabs.xz261.1gsar	48	140	0.2204E+00	0.3522E-02	55998
slabs.xz262.1gsar	48	140	0.2121E+00	0.3399E-02	55998
slabs.xz263.1gsar	48	140	0.2036E+00	0.3280E-02	55998
slabs.xz264.1gsar	48	140	0.1950E+00	0.3166E-02	55998
slabs.xz265.1gsar	48	140	0.1864E+00	0.3056E-02	55998
slabs.xz266.1gsar	48	140	0.1777E+00	0.2952E-02	55998
slabs.xz267.1gsar	48	140	0.1690E+00	0.2853E-02	55998
slabs.xz268.1gsar	48	140	0.1604E+00	0.2760E-02	55998
slabs.xz269.1gsar	48	141	0.1519E+00	0.2674E-02	55998
slabs.xz270.1gsar	48	141	0.1435E+00	0.2593E-02	55998
slabs.xz271.1gsar	48	141	0.1352E+00	0.2519E-02	55998
slabs.xz272.1gsar	48	141	0.1271E+00	0.2450E-02	55998
slabs.xz273.1gsar	48	141	0.1192E+00	0.2387E-02	55998
slabs.xz274.1gsar	48	141	0.1115E+00	0.2328E-02	55998
slabs.xz275.1gsar	48	142	0.1041E+00	0.2273E-02	55998
slabs.xz276.1gsar	48	142	0.9700E-01	0.2221E-02	55998
slabs.xz277.1gsar	48	142	0.9016E-01	0.2170E-02	55998
slabs.xz278.1gsar	48	142	0.8362E-01	0.2119E-02	55998
slabs.xz279.1gsar	48	142	0.7737E-01	0.2066E-02	55998
slabs.xz280.1gsar	48	142	0.7141E-01	0.2011E-02	55998
slabs.xz281.1gsar	48	143	0.6578E-01	0.1950E-02	55998
slabs.xz282.1gsar	48	227	0.6437E-01	0.1884E-02	55998

Name of Slice Data File	Peak SAR x and z coordinates		Peak SAR (W/kg)	Avg. SAR (W/kg)	Voxels in tissue
slabs.xz283.1gsar	48	226	0.6472E-01	0.1812E-02	55998
slabs.xz284.1gsar	48	226	0.6331E-01	0.1731E-02	55998
slabs.xz285.1gsar	48	226	0.6235E-01	0.1639E-02	55998
slabs.xz286.1gsar	48	226	0.6213E-01	0.1548E-02	55998
slabs.xz287.1gsar	48	226	0.5928E-01	0.1448E-02	55998
slabs.xz288.1gsar	48	226	0.5928E-01	0.1389E-02	55998
slabs.xz289.1gsar	48	226	0.5151E-01	0.1320E-02	55998
slabs.xz290.1gsar	48	226	0.5151E-01	0.1395E-02	55998
slabs.xz291.1gsar	48	226	0.5011E-01	0.1359E-02	55998
slabs.xz292.1gsar	48	226	0.5011E-01	0.1292E-02	55997

Location and values for peak and average SAR for total volume of exposed tissue

Slabs.xz232.sar	48	140	0.3464E+00	0.3604E-02	15567443

Figure 3.8 illustrates the orientation of the inhomogeneous slab model with respect to the antenna in xz plane at y = 81 mm from the origin of the rectangular coordinate system at the lower-front-left corner of the fdtd mesh. The horizontal black lines, A through C denotes the horizontal xy planes and the vertical black lines, D through N denotes the vertical yz planes where the SAR data was plotted and printed. Figure 3.9 illustrates the orientation of the inhomogeneous slab model with respect to the antenna in xy plane at z = 141 mm from the origin of the rectangular coordinate system. The horizontal black lines, O through Q denotes the vertical xz planes and the vertical black lines, D through N denotes the vertical yz planes where the SAR data was plotted and printed.

Figure 8.1 illustrates the SAR distribution in xz planes through the slab model corresponding to the vertical slices O (through the center of the left row of antenna patches), P (through the center of the array of patches) and Q (through the right row of patches) defined in Figure 3.9. The boundaries for the skin, fat and muscle are apparent in the color plots since the SAR is markedly different in each due to the different dielectric properties. Note that the maximum SAR occurs in the skin with significantly reduced SAR in the fat layer and increased SAR in the muscle near the fat-muscle interface, decreasing sharply with increasing depth into the muscle. The patterns show that the highest SAR occurs in front of the patches with the a maximum of 0.802 W/kg in front of the lower right patch at scan Q, slice 228. Figure 8.2 illustrates the SAR distribution in the xy planes through the slab model corresponding to the horizontal slices A (through the bottom row of patches), B (through the middle of the patch array) and C (through the top row of patches) defined in Figure .99. The maximum SAR for this case is 0.805 W/kg (highest for entire slab model) occurring in scan A, slice 141 adjacent to the lower right patch of the antenna.

Figures 8.3 and 8.12 respectively illustrate the SAR distribution in the vertical yz planes at slices labeled as D through M in Figure 3.9. The peak SAR of 0.790 W/kg for this series of scans occurs near the scan through the slice denoted as scan D or slice 50 in the skin layer in Figure 8.3. The black cross indicates the location of the FDTD cell in the layer experiencing the highest SAR. The maximum SAR of 0.805 W/kg in the entire model occurs in the adjoining layer at slice 49. Figure 8.4 indicates that the maximum SAR in scan E or slice 51 at the top of the fat layer is 0.0454 W/kg, a large decrease from that in the skin layer. Figure 8.5 indicates a further reduction of SAR to 0.0218 W/kg with increasing depth in the fat layer at scan F or slice 56. These values are consistent with the sharply lower electrical conductivity in the fat. Figure 8.6 shows a sharp increase of SAR up to 0.127 W/kg at increased depth into the model at scan G or slice 62 near the top of the muscle layer. This is consistent with the much higher electrical conductivity of the muscle. The remaining figures illustrating the SAR distributions in the yz planes show a rapid decrease of the maximum SAR with increasing depth as a result of the sharp decay of the SAR with distance into the

high conductivity muscle layer.

Figure 8.13 illustrates the respective color plots of the 1-gram average SAR distribution in the xz planes denoted by O through Q as identified in Figure 3.9. The legend for each plot is based on 0 dB = maximum 1 gram average SAR. Figure 8.14 illustrates the same plots as shown in Figure 8.13 except for the case the legend for all of the plots is set to allow the color red to represent all SARs at or greater than the value 1.6 W/kg allowed by the FCC MPL. Figure 8.15 illustrates the plots in the xz plane where the scans correspond to the locations of maximum SAR. From left to right, the first scan, slice 231 is that showing the maximum peak SAR of 0.805 W/kg for the entire model, the second scan, slice 232 is that showing the maximum 1 gram average SAR of 0.3464 W/kg for the entire model, set to correspond to 0 dB, and the third scan, slice 232 is the same as the second scan except 0 dB corresponds to the FCC MPL of 1.6 W/kg. A plus sign denotes the exact position of the maximum SAR for all scans. The maximum SAR is 6.6 dB below the FCC MPL.

The calculated maximum peak and 1-gram average SARs in the inhomogeneous slab model exposed while in contact with the radome compare reasonably close to the calculated values obtained by SPEAG for the homogeneous slab model discussed on pages 25 to 28 and in Sub-Appendix G of Appendix A. The values also compare favorably with measurements obtained by SARTest discussed in pages 5 through 25 of Appendix C. Typical calculated and measured values that relate to the slab models exposed under similar conditions, while in contact with the radome are graphically compared in Figures 8.16 and 8.17. The former figure illustrates the values for distances in the model varying from 30 to 190 mm from the groundplane while the latter figure is enlarged to better show the detail of the SAR distribution between 30 and 80-mm from the groundplane in the multi-tissue layers of the inhomogeneous model.

The calculated peak SAR curve displayed as blue in the graphs clearly shows the classical characteristics of SAR distributions in plane layered tissue models exposed to RF sources. In the direction of wave propagation through the model, beginning with the skin layer the SAR has a maximum value of 0.8 W/kg in the skin since it has a high conductivity and is separated from the source by only a lossless layer of air. As the wave propagates through the fat layer the SAR drops sharply because of an order of magnitude drop in conductivity. The SAR continues to decrease rapidly with distance within the fat due to three phenomena, (a) rapid decrease of the fields with distance from the source, (b) decay of the fields due to the lossy fat tissue and (c) the presence of a standing wave in the fat due to reflection from the high conductivity and permittivity muscle medium interface (null at location of fat-muscle interface). There is a sharp increase in SAR in the muscle tissue at the fat-muscle interface due to the order of magnitude increase in conductivity which is followed by a rapid exponential decay of the SAR with distance into the muscle layer. Finally near the backside of the model, standing waves appear due to the reflections from the muscle-air layer. The calculated 1-gram average SAR, displayed as a green curve, has a maximum value of 0.35 W/kg in the skin layer followed

by rapid decrease in value to 0.12 W/kg in the fat layer. The SAR then increases with distance into the muscle layer reaching maximum of 0.1 W/kg and finally decreasing with an exponential decay of 3 to 4 orders of magnitude near the backside of the slab. The red curve depicts the values of SAR measured by SARTest in the homogeneous phantom. The maximum value of these measurements was 0.275 W/kg at the interface of the simulated brain followed by an exponential decay with depth into the phantom. This peak is close to the maximum calculated 1-gram average SAR at the phantom interface. Due to the finite size of some measurement probes one can expect that the measured values of SAR would tend to be somewhere between the calculated values (averaged over a cubic mm) and the 1-gram average values. Note that the rate of decay is greater for the measured values than the calculated values, probably due to the fact that the conductivity of the tissue used for the former was 7 to 18% higher than that used for the latter. The curve depicting SARTest SAR measurements in the inhomogeneous slab model, shown in orange, has a maximum of 0.35 W/kg at the phantom skin interface, falls sharply in the fat layer to a low of 0.025 W/kg, rises to 0.075 W/kg in the muscle and finally decays very rapidly with distance into the muscle. The Peak SAR measured by SPEAG for the homogeneous model, shown as a red delta, was 0.860 W/kg, close to the calculated value of 0.805 W/kg for the inhomogeneous model. The maximum1-gram average SAR measured by SPEAG for the homogeneous model, shown as an orange delta, was 0.484 W/kg, somewhat higher than the 0.346 W/kg calculated 1-gram average for the inhomogeneous model. It may be concluded from these graphs that based on the work of three laboratories, the maximum 1-gram average SAR for the exposed slab tissue layers never exceeded 0.5 W/kg (5 dB below the FCC MPL).

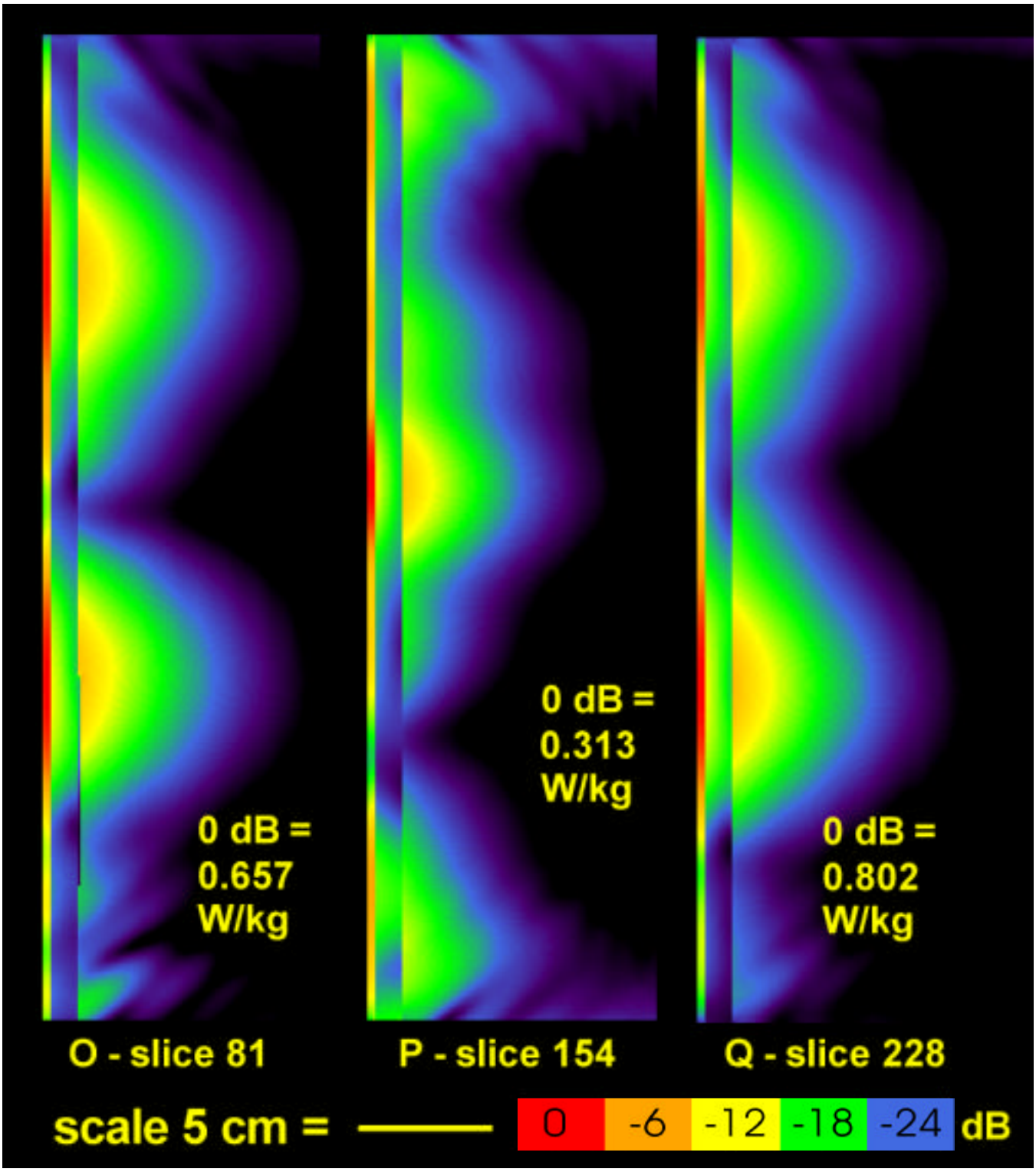

Figure 8.1. FDTD derived x-z plane SAR distributions (O-Q) in inhomogeneous slab torso model exposed to AT&T RU antenna.

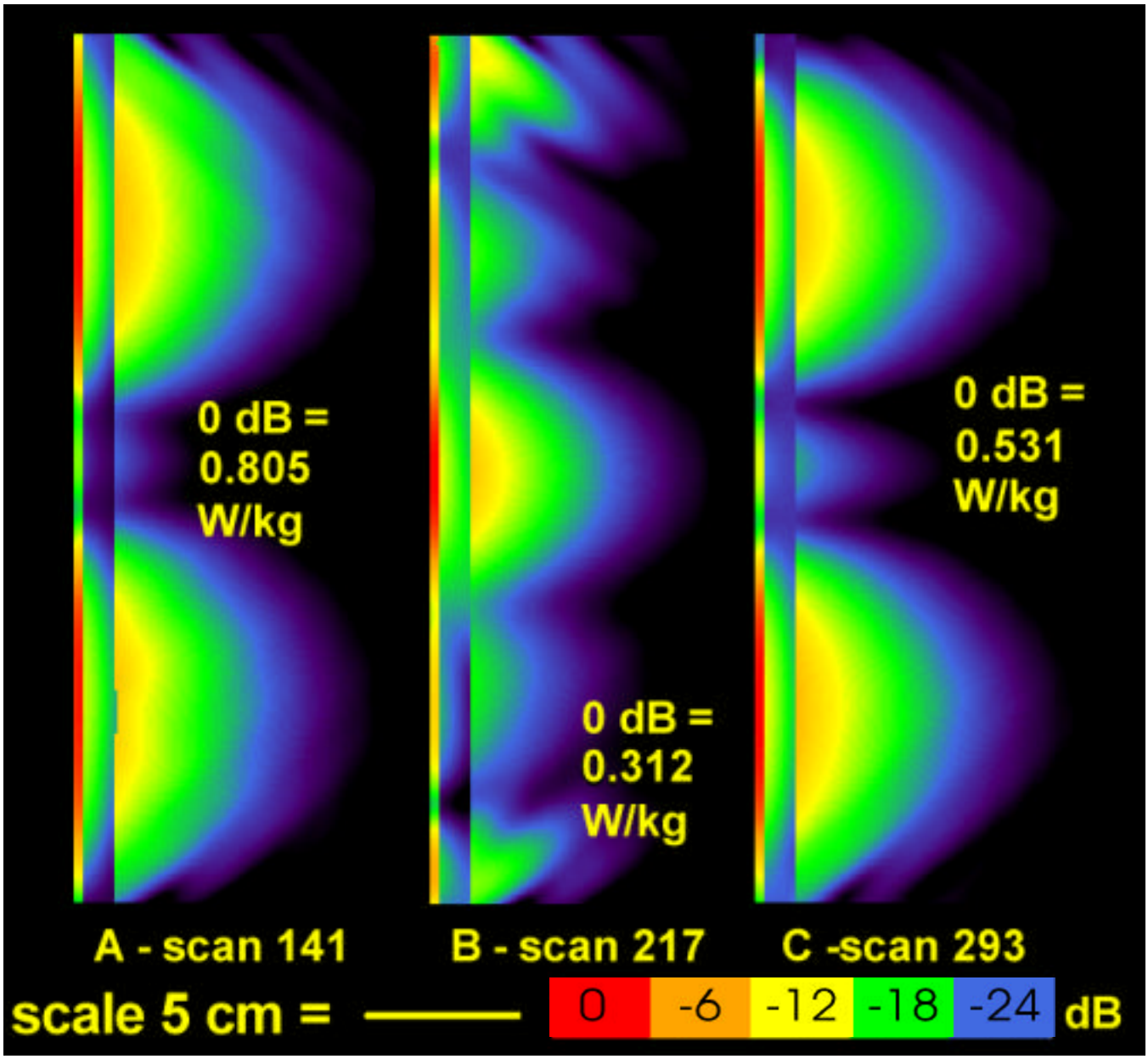

Figure 8.2. FDTD derived x-y plane SAR distributions (A-C) in inhomogeneous slab torso model exposed to AT&T RU antenna.

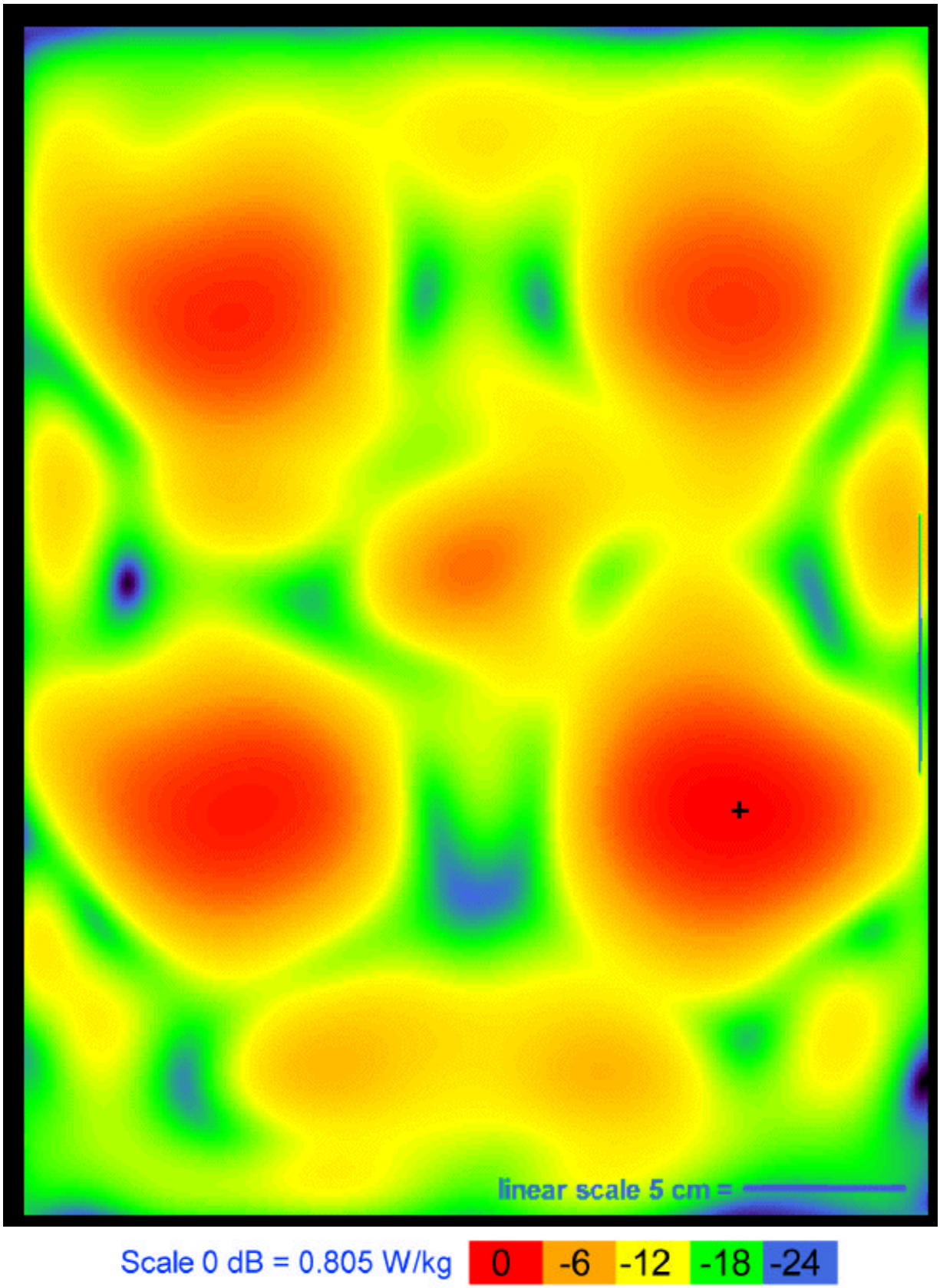

Figure 8.3. FDTD derived y-z plane SAR distribution at slice D - 50 in skin of inhomogeneous slab torso model exposed to AT&T RU antenna (black + indicates location of maximum SAR for entire model).

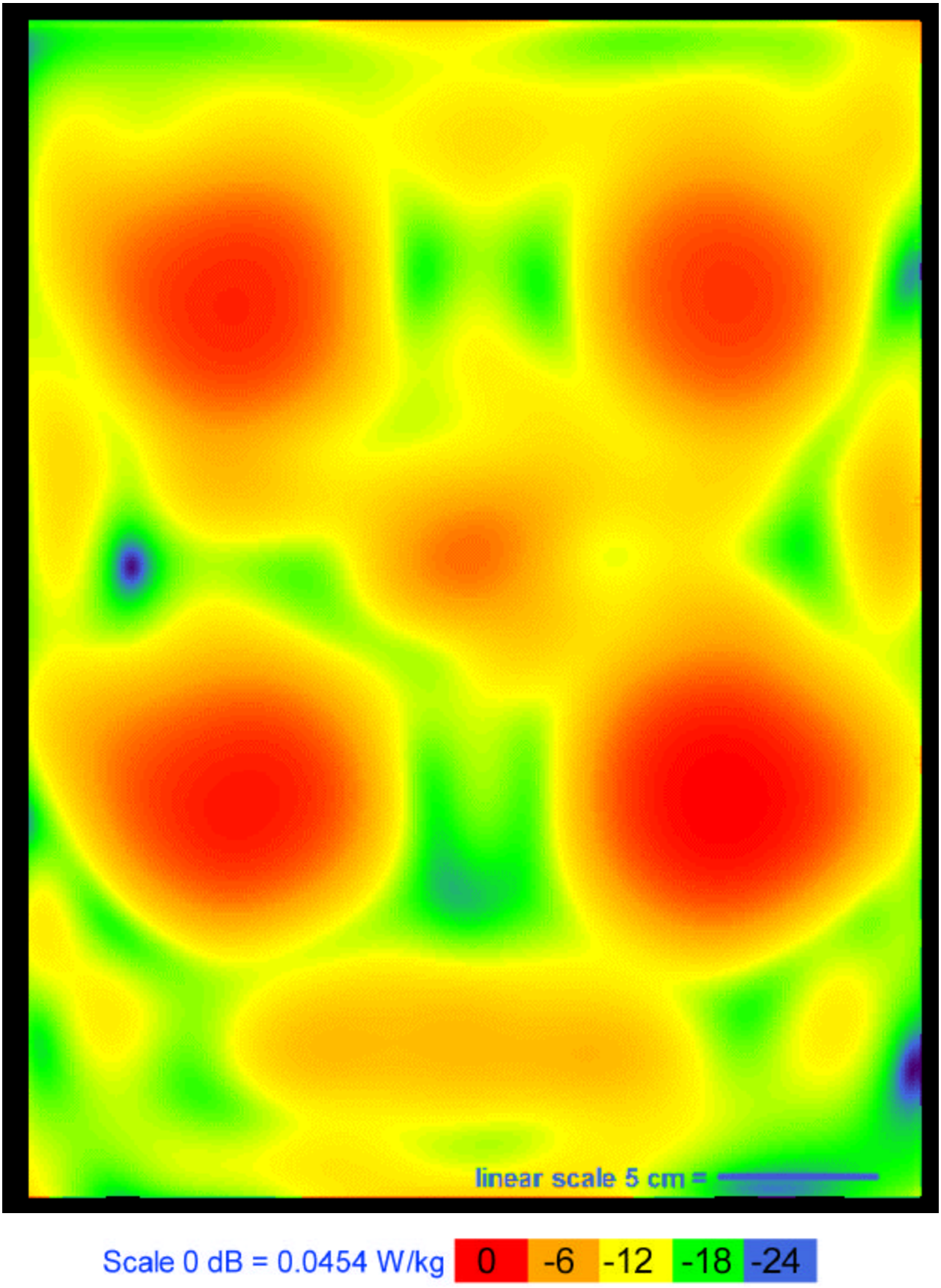

Figure 8.4. FDTD derived y-z plane SAR distribution at slice E - 51 in fat of homogeneous slab torso model exposed to AT&T RU antenna.

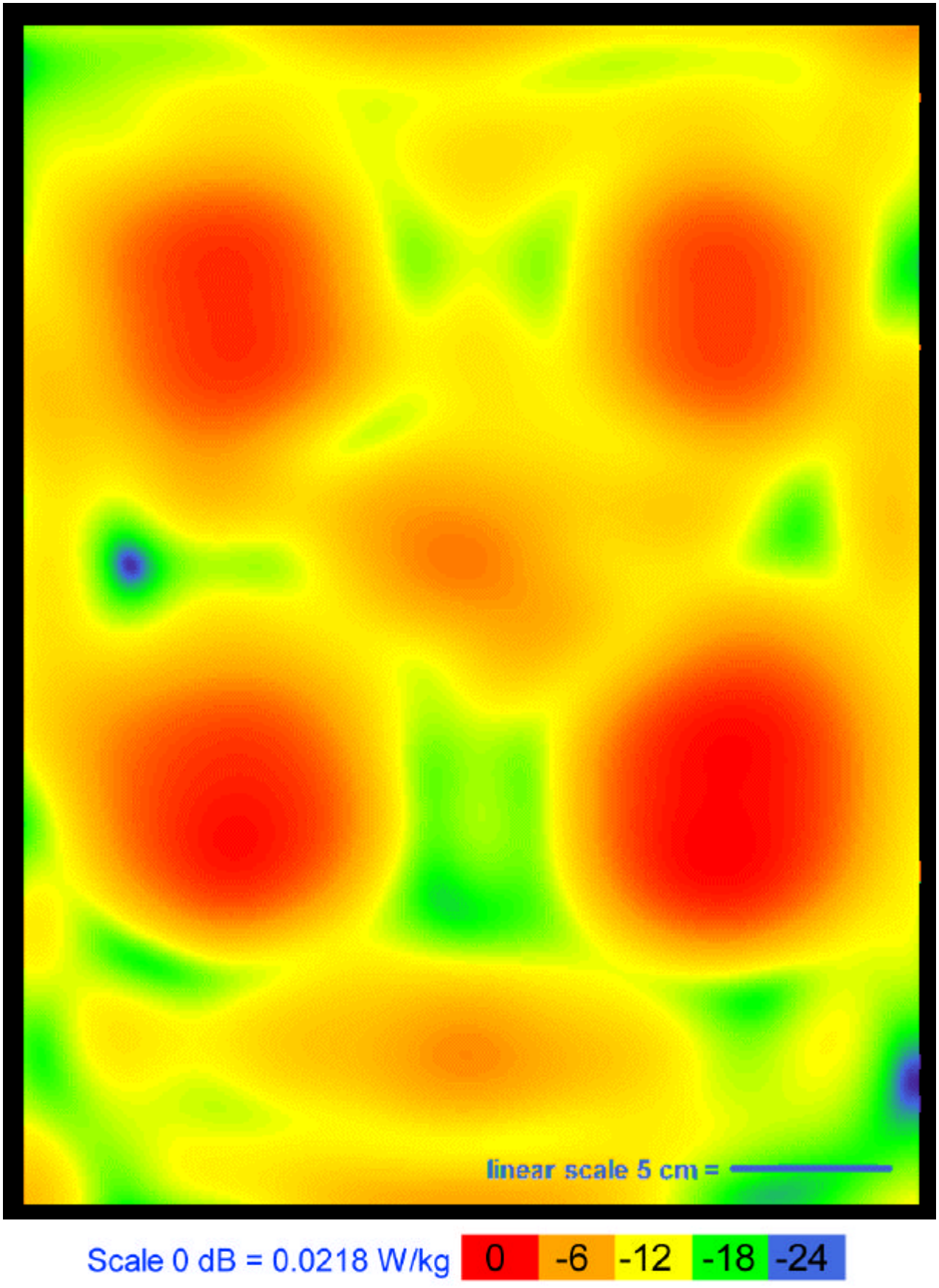

Figure 8.5. FDTD derived y-z plane SAR distribution at slice F - 56 in fat of inhomogeneous slab torso model exposed to AT&T RU antenna.

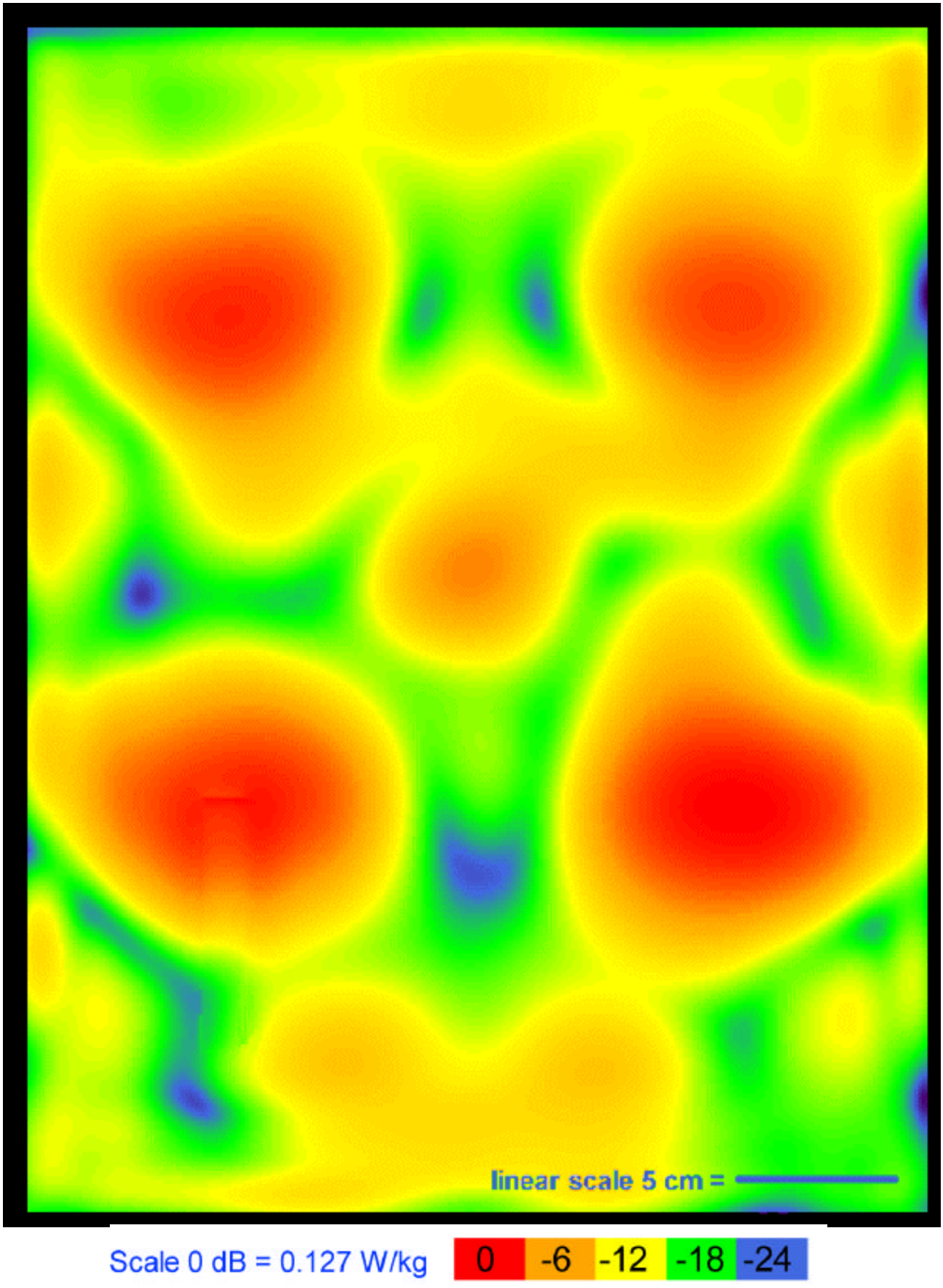

Figure 8.6. FDTD derived y-z plane SAR distribution at slice G - 62 in muscle of inhomogeneous slab torso model exposed to AT&T RU antenna.

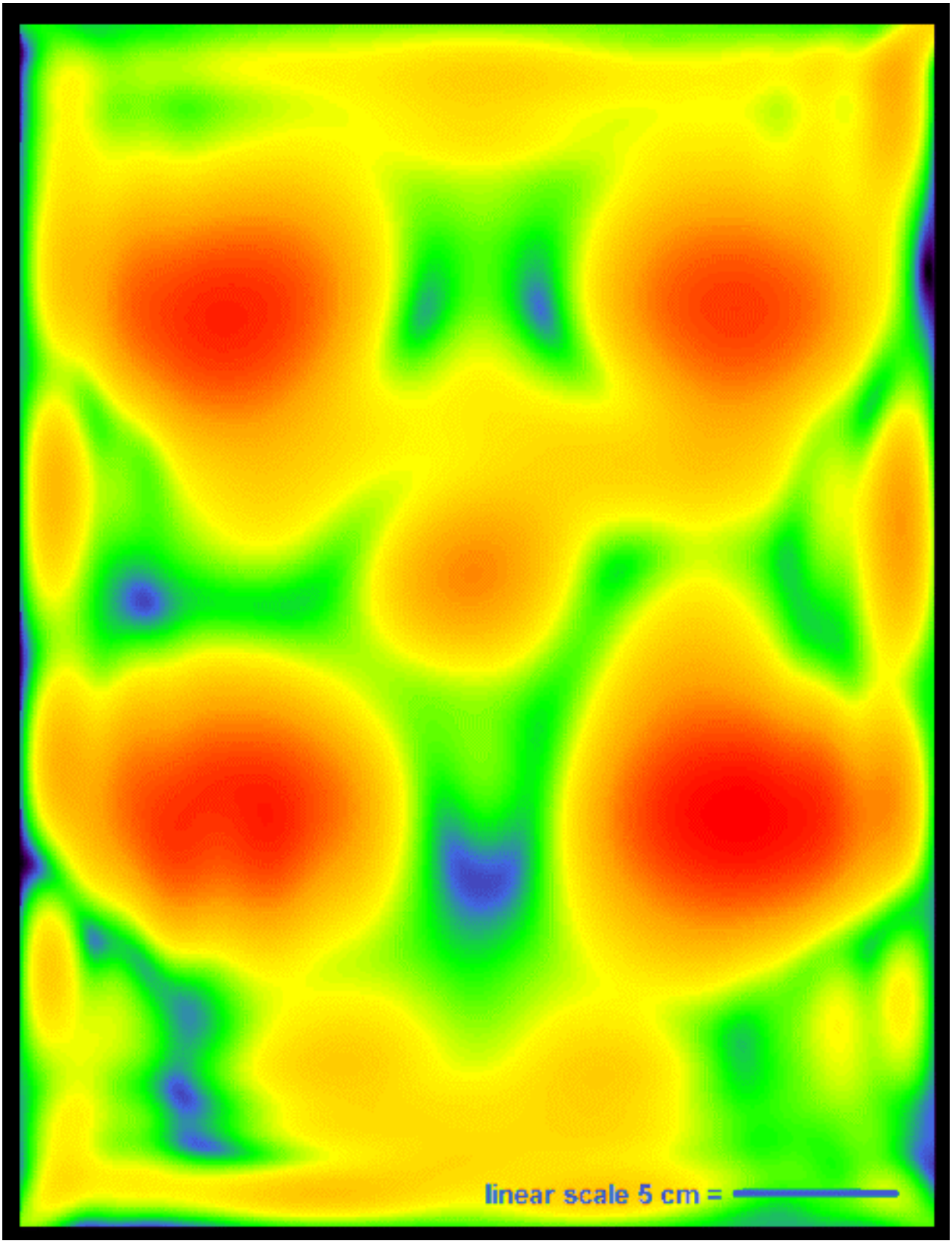

Figure 8.7. FDTD derived y-z plane SAR distribution at slice H - 71 in muscle of inhomogeneous slab torso model exposed to AT&T RU antenna.

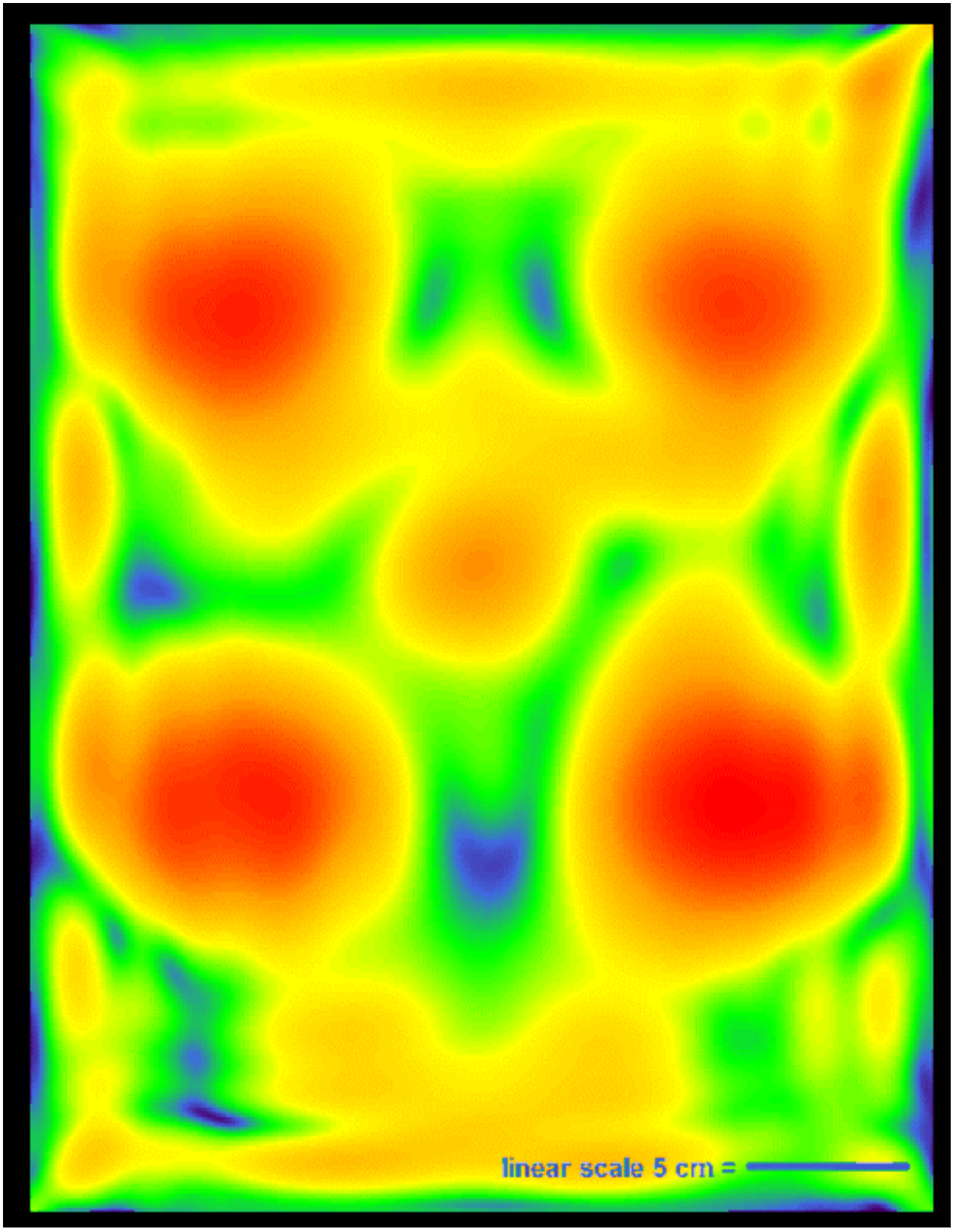

Figure 8.8. FDTD derived y-z plane SAR distribution at slice I - 80 in muscle of inhomogeneous slab torso model exposed to AT&T RU antenna.

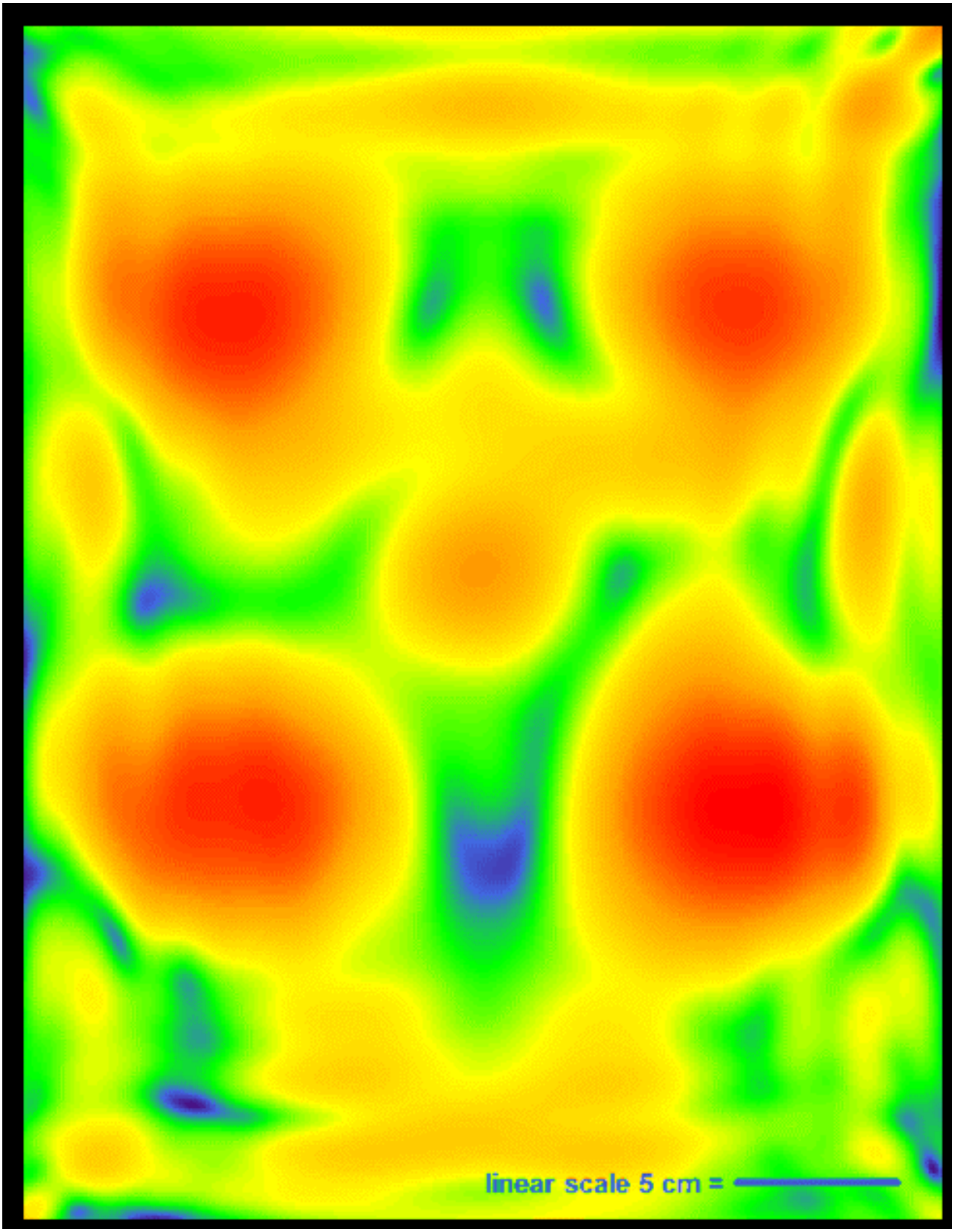

Figure 8.9. FDTD derived y-z plane SAR distribution at slice J - 90 in muscle of inhomogeneous slab torso model exposed to AT&T RU antenna.

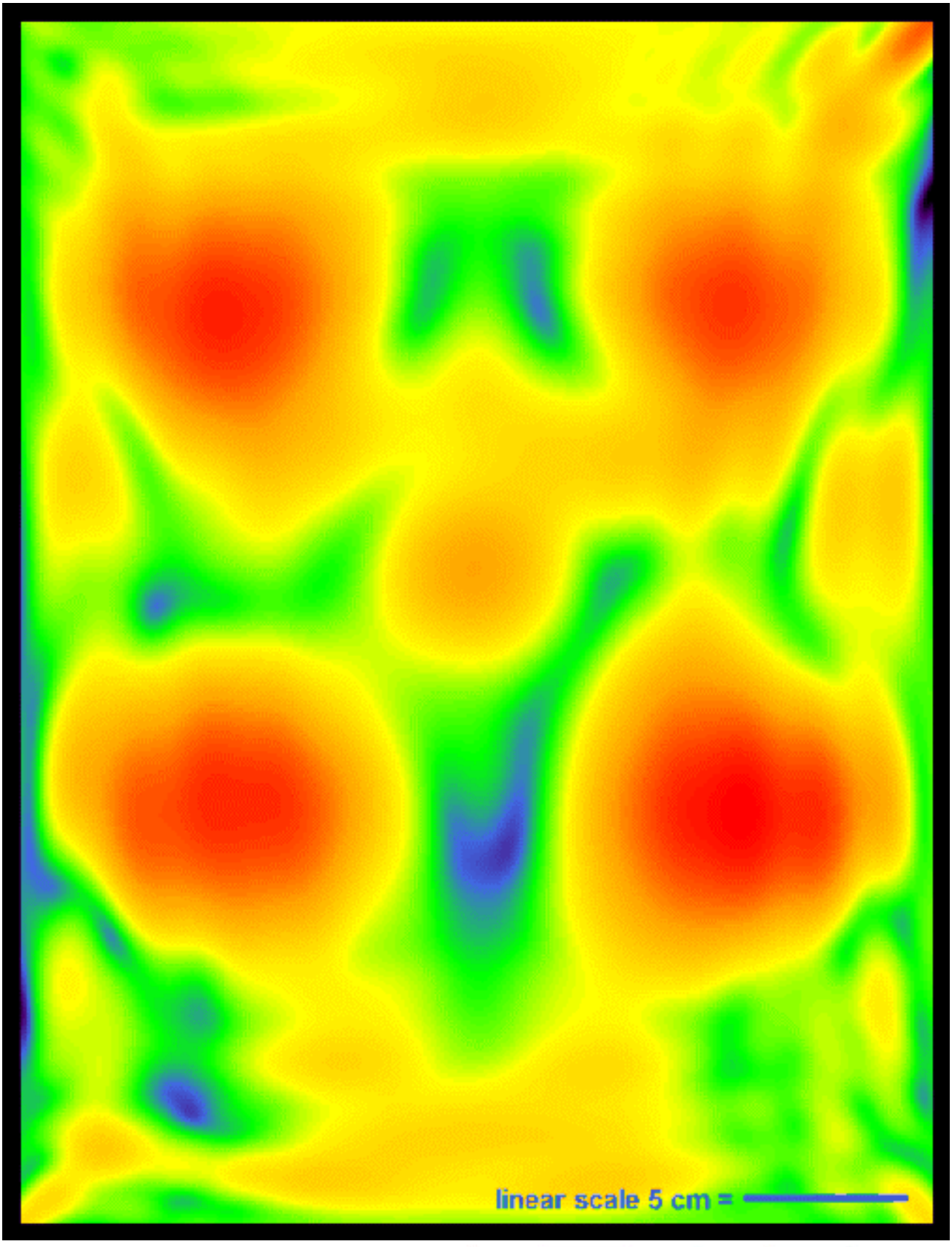

Figure 8.10. FDTD derived y-z plane SAR distribution at slice K - 100 in muscle of inhomogeneous slab torso model exposed to AT&T RU antenna.

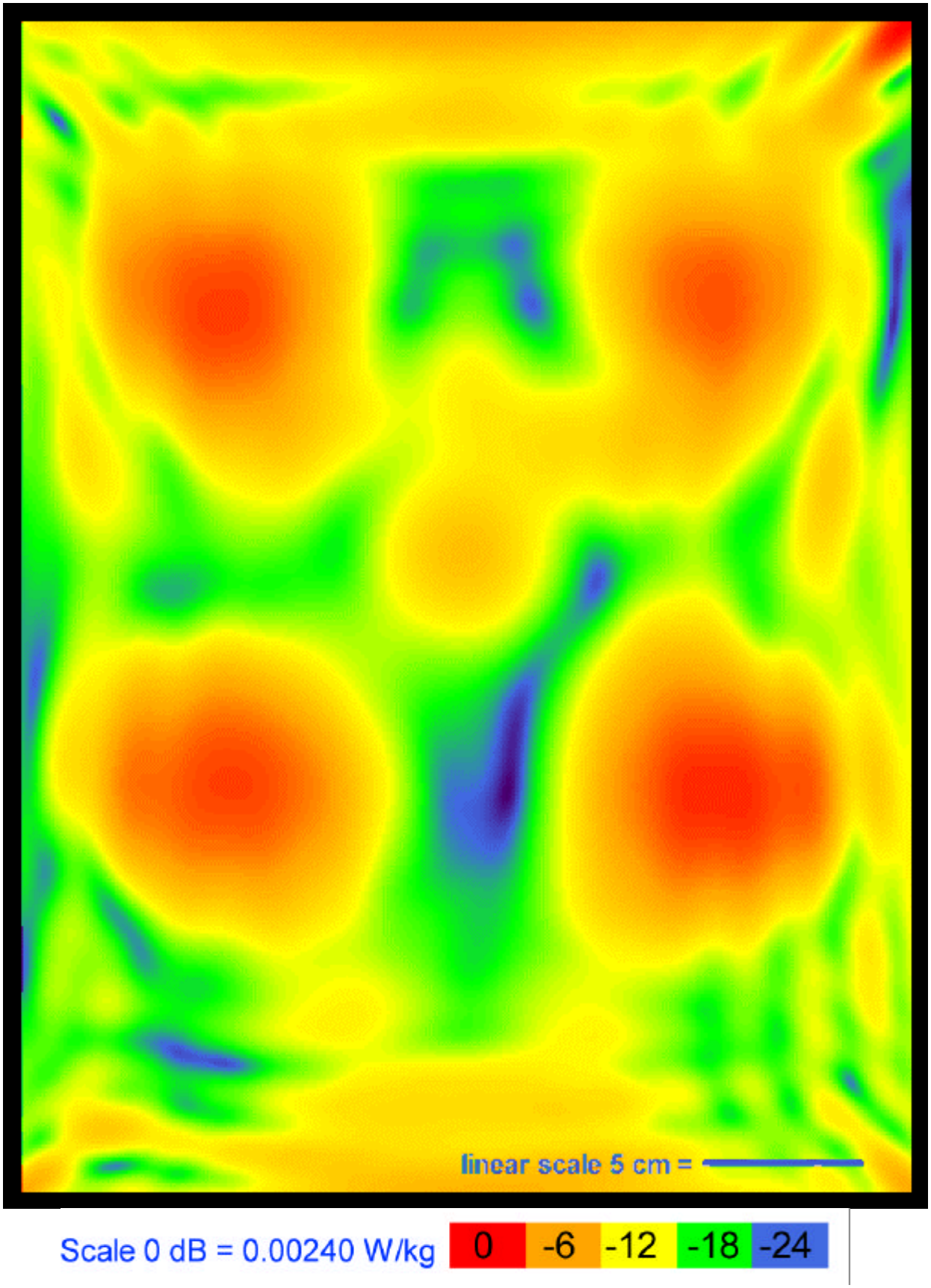

Figure 8.11. FDTD derived y-z plane SAR distribution at slice L - 120 in muscle of inhomogeneous slab torso model exposed to AT&T RU antenna.

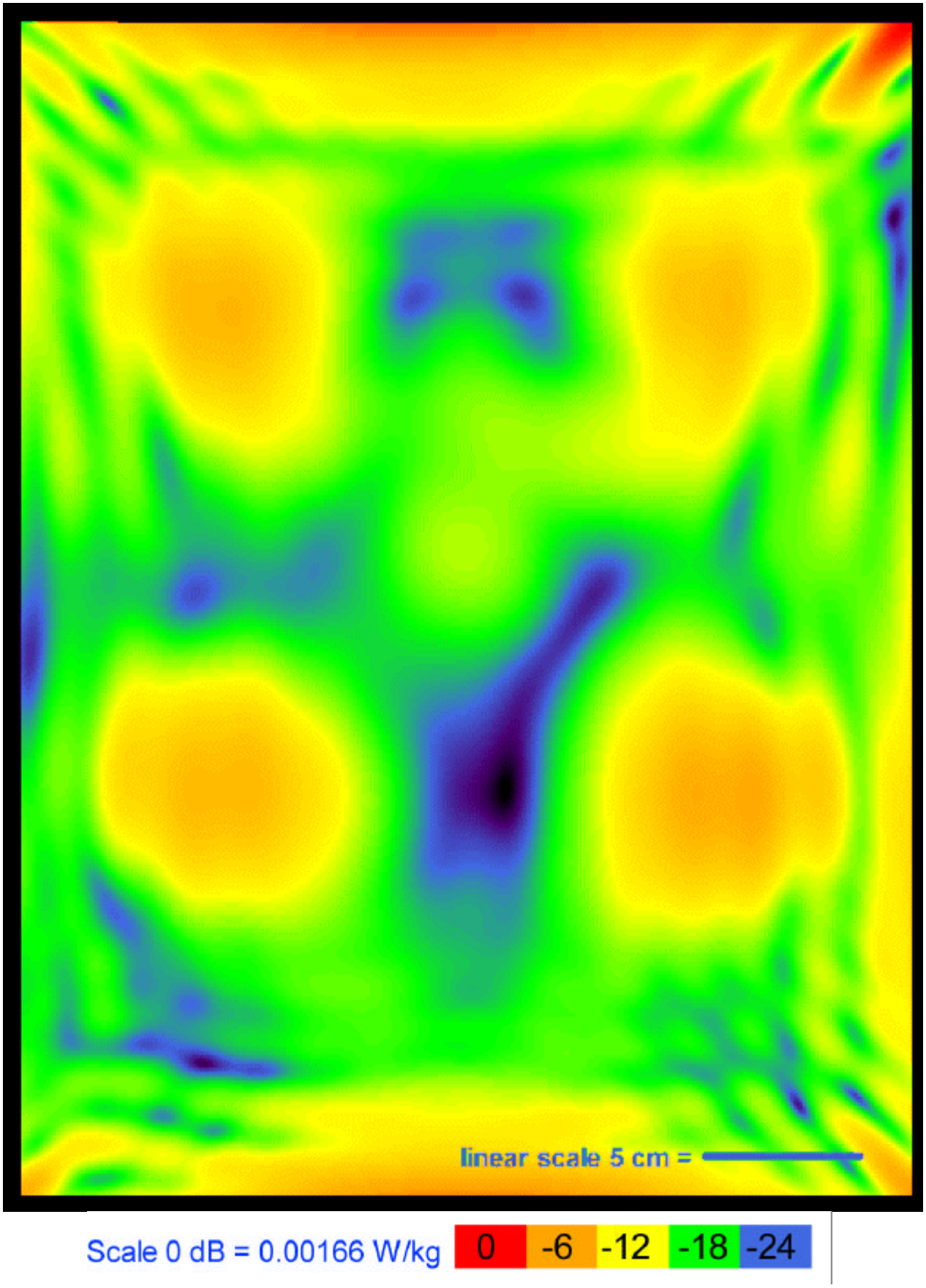

Figure 8.12. FDTD derived y-z plane SAR distribution at slice M - 140 in muscle of inhomogeneous slab torso model exposed to AT&T RU antenna.

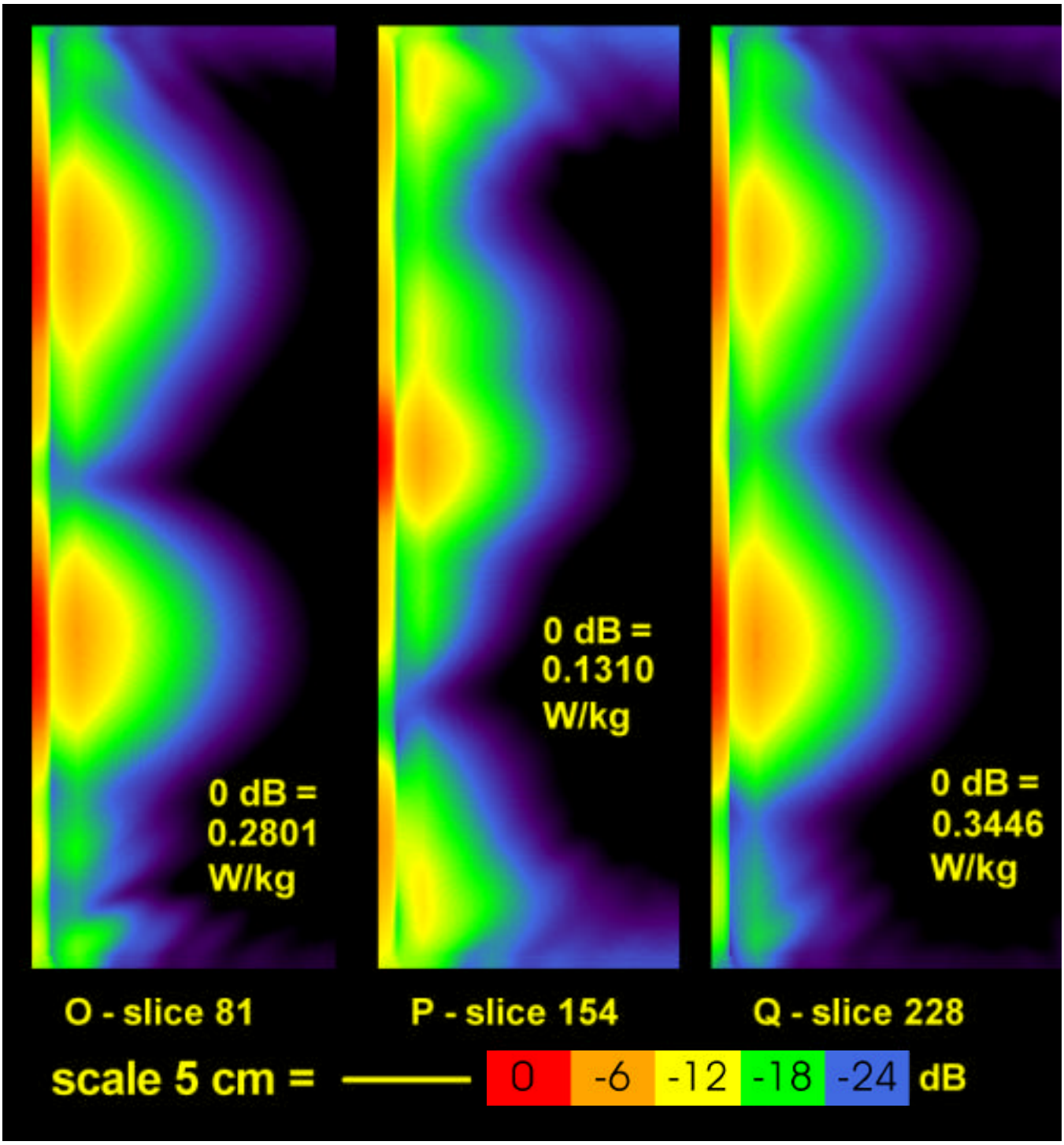

Figure 8.13. FDTD derived x-z plane 1 gram average SAR distributions in inhomogeneous slab torso model exposed to AT&T RU antenna.

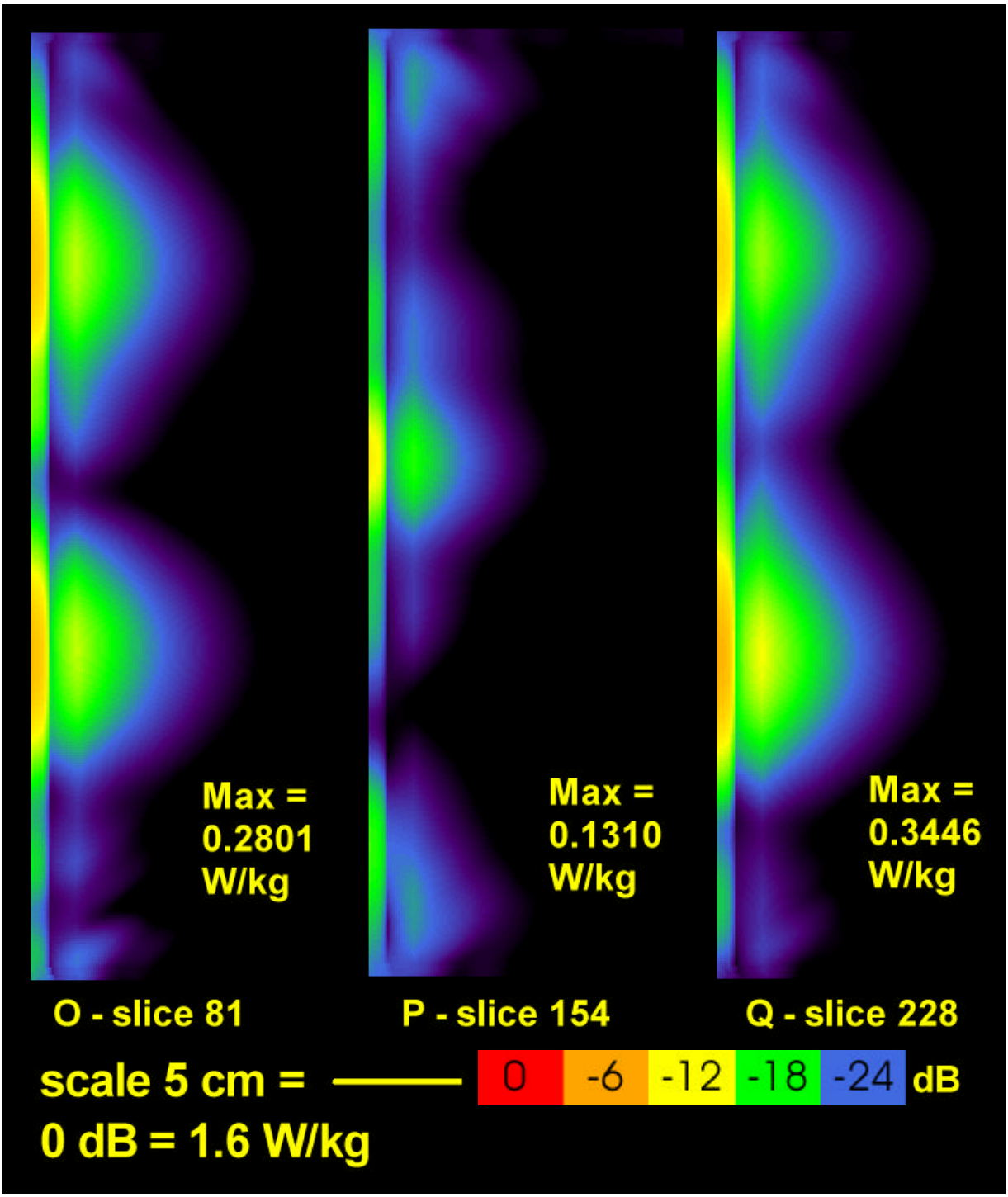

Figure 8.14. FDTD derived x-z plane 1 gram average SAR distributions in inhomogeneous slab torso model exposed to AT&T RU antenna compared to FCC MPL.

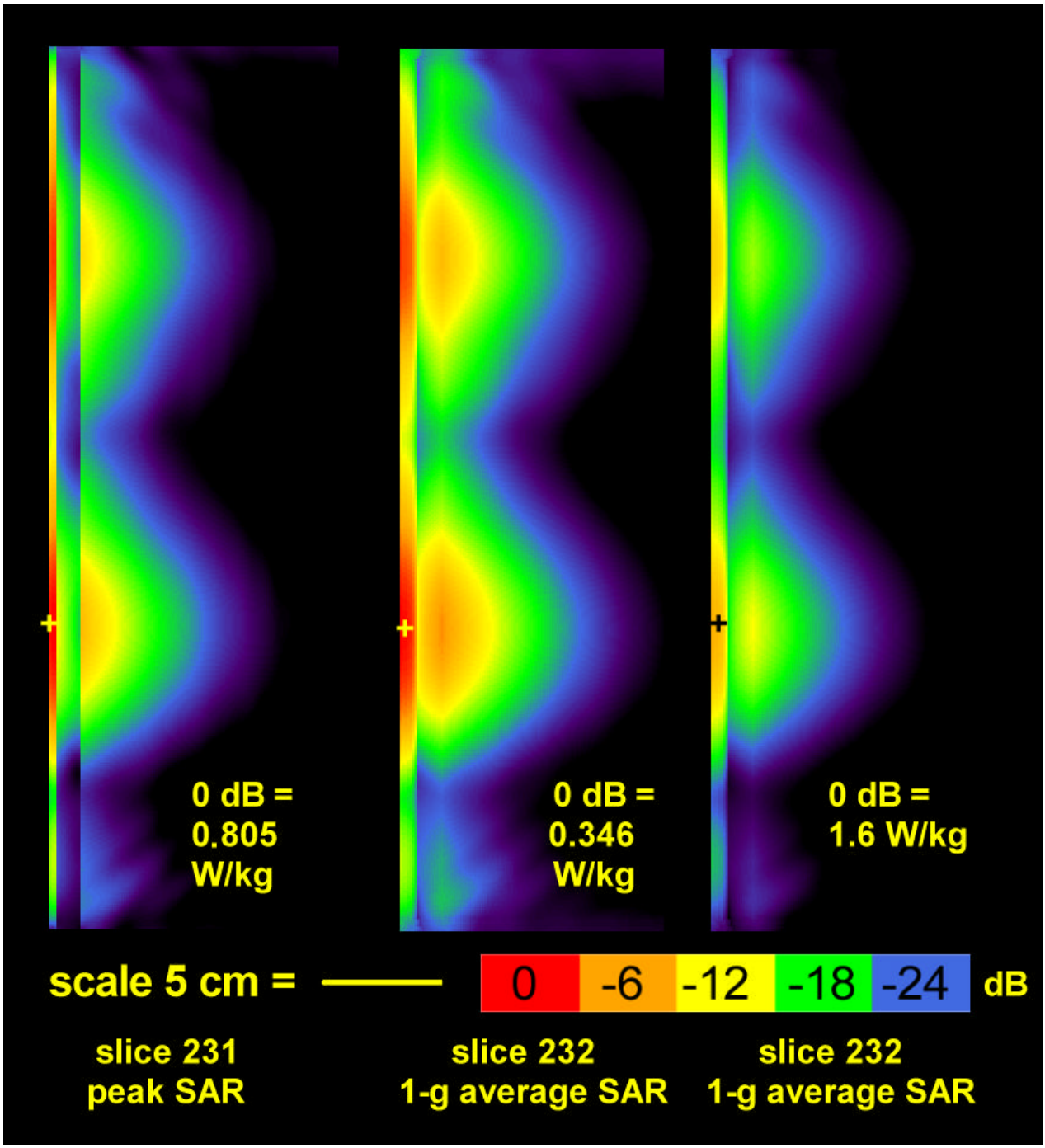

Figure 8.15. FDTD derived x-z plane scans from left to right, first slice 231 is that showing the maximum (0 dB) peak SAR of 0.805 W/kg for the entire model , second slice 232 is that showing the maximum (0 dB) 1 gram average SAR of 0.3464 W/kg for the entire model, and the third slice 232 is the same as the second slice except 0 dB corresponds to the FCC MPL of 1.6 W/kg (plus sign denotes the actual position of the maximum SAR 6.6 dB below the FCC MPL for all scans).